

C.S.Jeffery, N.T.Behara, C.Winter

Armagh Stellar Atmosphere Software
A Guide and Reference Manual

—

DRAFT - October 28, 2019

Contents

1	Introduction	11
2	Walkthrough	15
2.1	Installation: <code>ltecodes</code>	15
2.2	Installation: <code>wildcodes</code>	17
2.3	Making your first Model	18
2.3.1	<code>sterne</code>	18
2.3.2	<code>spectrum</code>	19
2.3.3	<code>sfit</code>	20
2.4	<code>condor</code>	21
3	Basic Assumptions	23
3.1	The SPECTRUM synthesis program	23
3.2	FFIT & SFIT	24
3.3	Validity of LTE Approximation	25
3.4	The Microturbulent Velocity	26
4	<code>sterne</code>	29
4.1	History	29
4.2	Radiative Transfer	31
4.2.1	Radiative transfer in a slowly expanding atmosphere.	32
4.3	Methods	33
4.4	The STERNE model atmosphere code	34
4.4.1	The Iterative Method	36
4.5	Opacity	38
4.5.1	Scattering	39
4.5.2	Free-Free Absorption	40
4.5.3	Bound-Free Absorption: Opacity Project Cross Sections	41
4.5.4	Bound-Free Absorption: IRON Project Cross Sections	43
4.5.5	Bound-Bound Absorption: Opacity Sampling	43
4.5.6	Wavelength Grid and Line Selection	47
4.5.7	Specifying the composition	48
5	<code>spectrum</code>	49
5.1	Formal Solution	49
5.1.1	Computational Accuracy	51

5.2	Line Profiles	51
6	Atomic Data	53
6.1	Hydrogen Lines	53
6.2	Helium Lines	53
6.3	Neutral Helium	54
6.3.1	Voigt profiles	54
6.3.2	Oscillator strengths for He I	55
6.3.3	Triplet splitting	55
6.3.4	Correction for ion collisions	55
6.3.5	Ion broadening	55
6.3.6	Forbidden components	56
6.3.7	Data required	57
6.3.8	Semiclassical impact line widths	57
6.3.9	Electron broadening in the impact approximation	57
6.3.10	Overlapping line theory	57
6.4	Ionized Helium	58
6.5	Metals: atomic data for stellar atmospheres	58
7	ltelines	61
7.1	Major sources	62
7.2	Programs	63
7.3	Individual line data for ltelines	63
8	idlines	65
8.1	Usage	65
8.2	Arguments	65
8.3	Keywords	65
8.4	Input Files	66
8.5	Prologue	67
9	ffit	69
10	sfit	71
10.1	sfit: solve	72
10.2	sfit: synth	72
10.3	Operation of the Programs	73
10.4	SFIT - some corrections – 2013	73

10.4.1	The fitting function	73
10.4.2	χ^2 minimisation and parameterisation	74
10.4.3	Features and Bugs	75
11	Dynamical atmospheres	77
11.1	Non-standard Line Profiles	77
11.1.1	Velocity Perturbations	77
11.1.2	Temperature Perturbations	83
A	SPECTRUM - command summary	87
A.1	General Commands	87
A.2	Parameter Definition	87
A.3	Model Atmosphere Input	87
A.4	Atomic Data	88
A.5	Abundances	88
A.6	Velocities, etc.	88
A.7	Radiative Transfer	88
A.8	Examples	89
B	ltecodes – walkthrough examples	91
B.1	example.spc	91
B.2	StnPG0909	93
B.3	SpcPG0909	95
B.4	sterneos.sh	97
C	isfit	107
C.1	sfit control file editor	107
C.2	Plot sfit output	111
C.3	Examples	111

Summary

All of the information we obtain about stars is provided by electromagnetic radiation. The photons we detect originate in the outermost layers, or atmosphere, of the star. In order to interpret stellar spectra, it is necessary to construct models which accurately represent the structure of a stellar atmosphere and the transfer of radiation from the stellar interior into interstellar space. For the study of helium stars and other stellar remnants, we in Armagh use several computer programs, of which **sterne**, **spectrum** and **sfit** are the most important.

sterne	Line-blanketed LTE model atmospheres
spectrum	LTE radiative transfer: formal solution
lte_lines	Linelists for spectral analysis
idl_lines	Tools for building a spectral atlas
ffit	Fit stellar flux distributions (one or two stars)
sfit	Fit hires spectrum for T_{eff} , $\log g$, n_i , $v \sin i$, for single and binary stars. n_i is the abundance of an arbitrary element. Also find abundances and v_{turb}
libraries	Subroutine Libraries

The accompanying figure illustrates the procedures, inputs and outputs used in the analysis of high-resolution optical spectra and broad-band spectrophotometry.

In addition, we maintain local copies of the well-known model atmosphere codes developed by Kurucz and Hubeny on an *ad hoc* basis:

atlas9	Line-blanketed LTE model atmospheres (Kurucz)
synthe	LTE formal solutions (Kurucz/Lester)
tlusty	Non-LTE model atmospheres (Hubeny & Lanz)
synspec	Non-LTE formal solutions

These programs are available to Armagh Observatory astronomers and run on local workstations. See CSJ for details of how to run the codes in Armagh. Archive versions of many of these codes are available from CCP7 ¹

¹CCP7 = Collaborative Computational Project No. 7 for the Analysis of Astronomical Spectra developed and maintained an extensive library of high-performance radiative transfer software from 1980 through to 2002. The library is still accessible at ccp7.dur.ac.uk.

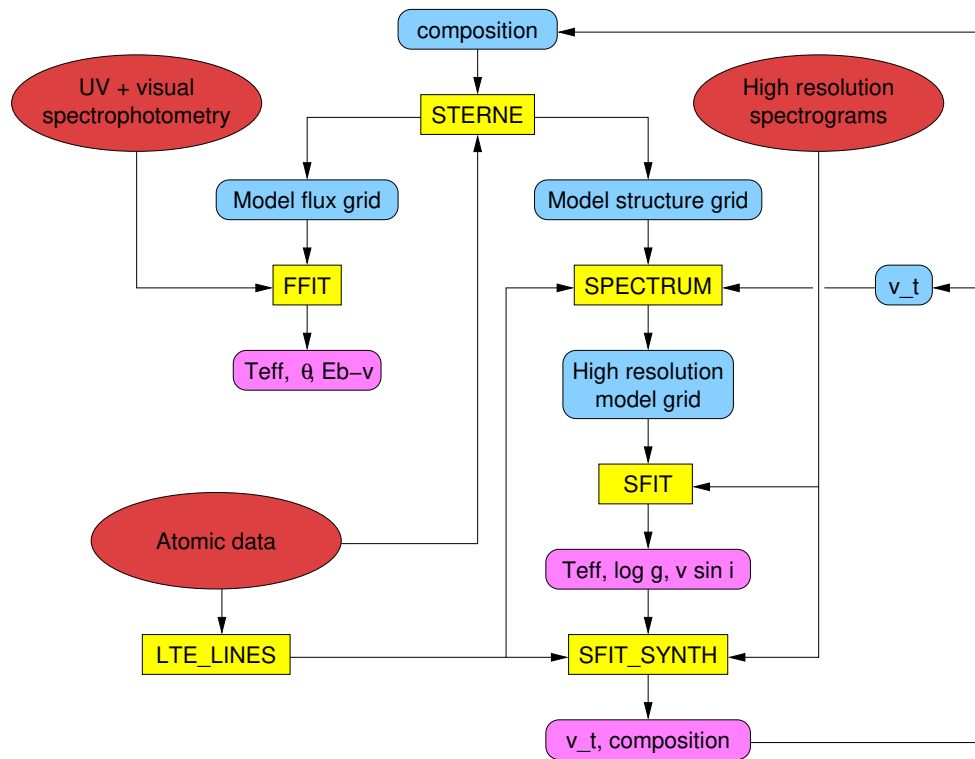


Figure 1: Block diagram illustrating the procedures (boxes), inputs (ellipses) and outputs (oval boxes) used in the analysis of spectra [Jeffery et al. \(2001\)](#).

1

Introduction

Essentially all the information we obtain from the observations of stars is provided by their electromagnetic radiation, and rests on our ability to correctly interpret their spectra. The STERNE code and the associated stellar atmosphere software at Armagh Observatory, which include SPECTRUM, FFIT and SFIT, provide us with the necessary tools to analyze stellar spectra. These programs are designed and used for the study of evolved stars, such as helium-rich stars and chemically peculiar subdwarfs. Starting with either a high-resolution optical spectra or low-resolution spectrophotometry, this group of programs allows us to determine various physical quantities, such as the chemical composition, effective temperature, surface gravity, angular radius and the interstellar extinction.

This chapter describes briefly the main functions of the principal programs in the collection. The physics associated with each code is described in subsequent chapters. Details of how to operate the programs are provided on the website: <http://star.arm.ac.uk/~csj/lte-codes/>
sterne: a program which calculates the structure of stellar atmospheres. It is optimized for stars with effective temperatures between 10,000 and 35,000 K, and is specifically designed to be suitable for the calculation of model atmospheres with extreme compositions dominated by helium, carbon and nitrogen.

The program assumes that the stellar atmosphere is plane-parallel and in local thermal, radiative and hydrostatic equilibrium. It considers opacities due to photo-ionization of all major ions and to approximately 10^5 lines. The original code was written by ? in Berlin, and has been substantially improved since by Heber (Kiel and Bamberg) and Jeffery (St Andrews and Armagh). A grid of model atmospheres computed using Sterne is also available.

spectrum: a spectrum synthesis program written originally by Philip Dufton (Queen's University Belfast) and subsequently extended by Danny Lennon, Liz Conlon (QUB) and Simon Jeffery (St Andrews and Armagh). The program has the following features:

- optimized for B-type stars, but has also been used with care(!) for cooler stars.

- a fast mode with a simple approximation for the source function ($S_\nu = B_\nu$) which is accurate for main-sequence stars and subdwarfs,
- a more general mode where the source function is solved for explicitly with scattering terms included.
- three sets of photoionization opacities for use with either, ATLAS, STERNE or STERNE3 model atmospheres.
- the code can generate:
 - equivalent widths and line profiles for individual lines
 - elemental abundances from line equivalent widths
 - curves of growth for individual lines
 - synthetic spectra over substantial wavelength intervals
 - equivalent widths for all lines in a given wavelength region
- several databases of linelists (e.g. LTE_LINES) and model atmospheres are available for use with the program.

lte_lines: a database of atomic data for, mostly, blue-visual absorption lines of light elements. Used primarily for calculating model spectra of early-type stars in LTE. The data is sorted with one file for each ion.

For each absorption line included, the database includes the wavelength, oscillator strength, radiative and collisional damping constants (where available), the excitation energy of the lower-level in the transition, the multiplet number (from Moore's revised multiplet tables). A reference for each of the oscillator strengths and damping constants are also given. The database is dynamic, with new lines being added as required. Some vetting is applied to ensure that only the most reliable data are included.

idlines: a suite of IDL tools to facilitate line identification and the interpretation of synthetic spectra. These allow for the construction of a spectral atlas showing an observed and synthetic spectrum at two scales, identified line locations from multiple atomic spectra and individual line identifications (including multiplet numbers) from individual atomic or ionic spectra. The tools are ideal for working with LTE_LINES format linelists and SPECTRUM output, but may be easily modified.

ffit: locates the best-fit model to an observed stellar spectral energy distribution. The latter is defined primarily by a star's effective temperature T_{eff} , angular diameter θ , and by interstellar extinction, characterised by the colour excess E_{B-V} . Given a grid of energy

distributions as a function of effective temperature, and a suitable description of the detected energy distribution, FFIT uses a χ^2 -minimization approach to solve for some or all of T_{eff} , θ and $E_{\text{B-V}}$. Several methods are available to solve the weighted multivariate χ^2 minimization problem, including the Levenburg-Marquardt method and a downhill simplex method (AMOEBAs).

In a binary star system, the apparent spectral energy distribution is determined the effective temperatures and angular diameters of both stars, $T_{\text{eff},1,2}$, and $\theta_{1,2}$, as well as by the interstellar extinction $E_{\text{B-V}}$, (assumed to be common to both stars).

FFIT (previously TFIT and BINFIT) will fit the spectral energy distribution of one or two stars. Model fluxes are either matched to specified spectral energy distributions or convolved with appropriate filter functions to match optical or infra-red broad-band fluxes. // **sfit**: At higher resolution, the spectrum of a star is defined primarily by its effective temperature T_{eff} , its surface gravity g and its chemical composition. Absorption lines are also modified by rotational and microturbulent broadening. Given a grid of high-resolution spectra, such as those computed with spectrum, these programs locate a best fit in T_{eff} , $\log g$, v_{turb} and one other variable (eg helium abundance or metallicity). sfit was completely revised in 2004 October.

After fixing T_{eff} , $\log g$, v_{turb} , and, possibly, helium abundance, it may be desirable to compute the abundances of other individual chemical species. However the number of independent parameters now becomes so large that precomputing large grids for multivariate analysis becomes prohibitive, especially when it is desirable to include several hundreds of spectral lines. This program computes a synthetic spectrum for a given starting composition, and then uses a search algorithm (AMOEBAs or LEVENBURG) to find the best solution for those parameters that are allowed to vary, recomputing the best fit spectrum as it goes. // **synthe**: A spectrum synthesis program written originally by Bob Kurucz and used in conjunction with his programs atlas, balmer and width. It was adapted by John Lester and made available through CCP7 by Simon Jeffery - who added a number of scripts to make file management more straightforward.

In Armagh, the code has been used in studies of the cool companions of sdB binaries for which a modest model grid has been computed. // **libraries**: The principal codes described above (**sterne**, **spectrum** and **sfit**) use a number of subroutine libraries with a wide range of utilities. Some of these are described in more detail in accompanying documentation. All of the libraries are bundled with the distributed version of the codes.

2

Walkthrough

Chapter author: **James Wild**

This is the chapter you need if you just want to get **ltecodes** installed and running for a straightforward example. It is intended to walk you through the necessary steps and will assume you are running on a UNIX system, i.e. either OS X or your preferred flavour of GNU/Linux.

2.1. Installation: ltecodes

- Install the gfortran compiler, or an equivalent. [The official docs will help here](#). On Ubuntu:

```
sudo apt-get install gfortran -y; echo -e '\n\n\n'; gfortran --version
```

- Download/obtain the latest LTECODES version. At time of writing, this is v3.2.5.
- Extract the files into a directory. The location doesn't matter, but it's preferable to put it in your home directory.
- Configure the FORTRAN file. Navigate to the directory you put **ltecodes** with the terminal, and execute the following command:

```
mkdir $HOME/LTECODES; sudo ./configure -prefix=$HOME/LTECODES
```

This will create a directory, and set maketools to install LTECODES to it.

- Now we must make the files. The following commands will scrub the existing files, make new ones, and test the result:

```
make clean; make install
```

- This should take a few minutes to execute. When it's finished, navigate to the directory and test the code installed correctly.

```
cd $HOME/LTECODES/bin; ./sfit
```

This should start **sfit** in command line mode. Type 'end' to exit the interface.

- Now we must edit out PATH variable to include this folder. you can check your path by entering:

```
echo -e "\nPATH VARIABLE:\n${PATH}\n\nHOME DIRECTORY:\n${HOME}\n"
```

- Adding a new directory to the path is different depending on your system. I'll briefly outline how to do it on OS X and Ubuntu as examples.

- OS X: The path is defined in \$HOME/.BASH_PROFILE. You can easily append the required directory with:

```
echo -e '\n# Add LTECODES to the path' >> $HOME/.bash_profile
echo -e 'export PATH=$PATH:$HOME/LTECODES/bin' >>\
$HOME/.bash_profile
echo -e '# Add LTECODES path for grabbing data from files' >>\
$HOME/.bash_profile
echo -e 'export LTECODES=$HOME/LTECODES' >> $HOME/.bash_profile
```

- Ubuntu: The method is identical, however the file is named differently, and depends on how we use the code. For simplicity, I recommend using \$HOME/.PROFILE. NOTE: If \$HOME/.BASH_PROFILE or \$HOME/.BASH_LOGIN exist, then .profile is NOT loaded. If you have issues, google is your friend.

```
echo -e '\n# Add LTECODES to the path' >> $HOME/.profile
echo -e 'export PATH=$PATH:$HOME/LTECODES' >> $HOME/.profile
echo -e '# Add LTECODES path for grabbing data from files' >>\
$HOME/.profile
echo -e 'export LTECODES=$HOME/LTECODES' >> $HOME/.profile
```

- Now, navigate to an unrelated directory and type `sfitto` to check that everything worked.
- Finally, obtain the tarball of `ltecodesshare` data. This can be found with Simon Jeffery (`csj@arm.ac.uk`). Extract this and place it in the share folder.

2.2. Installation: wildcodes

- Make sure you have python 2.7 with `PYTHON -VERSION`. If you get back python 3.x, most of the scripts will be incompatible. You can get python with:

```
sudo apt-get install python2.7 -y
```

The scripts also rely on Tkinter, [so make sure you have it installed](#)

- Download the codes from [GitHub](#), and extract the files into a folder.
- Navigate to the folder, and run `SUDO ./SETUP`. This creates symbolic links to the scripts in your bin to make them accessible as commands in the terminal, and checks you have all the pre-requisites.
 - If this doesn't work, it can be done manually. Add the wildcodes folder to your path, and navigate to it. Run `CHMOD +x ./*` to make all the scripts executable. The scripts have some python dependancies, a list of which is in the `SETUP` script.
- Test the scripts have installed correctly by running `CD $HOME; WILDLINES`. The terminal should resize, and ask for an input from the user. Pressing the 'n' key should print out the controls.

2.3. Making your first Model

2.3.1. sterne

The first step is to generate a **sterne** model atmosphere. This is best done with STERNEOS, as it requires the least work for a single model. This is done by first generating an input model, with the following command:

```
SterneOS.input <T> <logg> <ND> <nH> <nHe> <nC> <nN> <nO> <xSi> <xCa> <xFe>
  <grey> <last> <model name> [niter]
```

For this command, we have the following arguments:

- Teff: K : Effective Temperature
- logg: cgs: Surface Gravity
- ND : : Number of depth points in the atmosphere
- nH : : Hydrogen Abundance: fractional by number
- nHe : : Helium Abundance: fractional by number
- nC : : Carbon Abundance: fractional by number
- nN : : Nitrogen Abundance: fractional by number
- xO : : Oxygen number fraction: Scale factor: 1.0 = solar
- xSi : : Silicon ++ number fraction: scale factor: 1.0 = solar
- xCa : : Calcium ++ number fraction: scale factor: 1.0 = solar
- xFe : : Iron ++ number fraction: scale factor: 1.0 = solar
- grey:
 - 0 : start model from grey atmosphere
 - 1 : start model from partially converged atmosphere
- last:
 - 1 : grey or converged model as starting approx.

- >1 : converged model as starting approx with new parameters
- root: : name to use as root for all datafiles
- niter: : maximum number of iterations

Adjust your parameters accordingly. Note that the 4 number fractions must sum to 1 in order to be valid. The four scaled elements are scaled relative to the sun BY NUMBER, or if we are looking at abundances (ϵ) then e.g. $x_{\text{Si}} = 10^{\epsilon_{\text{Si}} - \epsilon_{\text{Si},\odot}}$.

After running this command, you should now have a new file in whatever directory you ran the command from with the name <MODEL NAME>. Typical values for niter are about 150, however if the model fails to converge within this, bump up the number. I've not had a model take more than 300 iterations, as a reference point.

Now we can run **sterne**. There's a script in the appendix that makes running **sterne** much smoother, **STERNEOS.SH**. Copy and paste this into your **ltecodes** bin and make it executable (`SUDO CHMOD +X STERNEOS.SH`). Supply the program with the input file you just generated with the following command:

```
sterneos.sh <root>
```

This should generate a *.Q, *.S, and *.T file. These contain the profiles for **spectrum** to use.

2.3.2. spectrum

spectrum takes the generated profiles from **sterne** and creates an emergent spectrum from them. It is often bypassed with **sfit**, however we will briefly outline its use.

Along with the models generated with **sterne**, **spectrum** has a few requirements. We need a line list containing atomic data, and an input.spc file. A line list can be generated using the scripts contained in **wildcodes** `READ_XXXX`.

An spc file can do four basic things; generate a spectrum (`CALC_SYNT`), calculate the theoretical equivalent widths of lines (`CALC_LINES`), calculate a specific line profile (`CALC_PROF`), or try and find the abundance of an element (`CALC_ABUND`). The comment character is a !. The structure of an spc file is as follows:

1. Define the data sets (unless using the defaults). This often doesn't need to be done.
2. Read in the atmospheric model and line data
3. Define the abundances (if synthesising a spectrum) or define the abundances you wish to determine with `ABUND <Z> <X>`, or `CALC_ABUND <Z> <X> <TOL>`

4. Define the physical parameters of the star, such as `VSINI <X>`, `VRAD <X>`, and `VTURB <X>`
5. Execute the function you want, `CALC_SYNT`H, `CALC_LINES`, `CALC_PROF`, or `CALC_ABUND`.

An example `.spc` file is in the appendix.

Run `spectrum` with the following command syntax:

```
spectrum.sh <model name.q> <linefile> <input file.spc> <output_name>
```

This will generate a `.FLUX`, `.FCON`, and `.XXX` files. The `.XXX` files will contain the `CALC` outputs, numbered sequentially.

2.3.3. `sfit`

`sfit` begins with an input model and line list. Then, an input (`*.sfit`) file is written, and fed into `sfit` for processing. The anatomy of an `sfit` input file is similar to the `*.spc` files above:

1. Define a model. This is done with `STERNE <MODEL NAME.Q>`
2. Define what input spectral data we want to use with `DATA_SPECTRUM <NAME>`, and the wavelength range we want to use.
3. Define any masks we want to apply to the data
4. Define what abundances we want to optimise. `ABUNDANCE <Z> <TOL>` – `tol` is the convergence threshold, typically 0.1 will work
5. Define velocities, and whether we want to vary them. There are 3 important ones, `SYN_VRAD1 <V> <TOL>`, `SYN_VSINI1 <V> <TOL>`, and `SYN_VTURB <V> <TOL>`
6. Define the method we want to use (I pretty much always use levenburg) with `METHOD_XXX`. e.g. `METHOD_LEVENBURG`
7. Set the program running with `SYNTH`.

`sfit` will then attempt to optimise the variables you've asked it to. `< tol >` is the flag to vary a parameter, and if it's set to 0.0, that parameter will be treated as a constant. A complete list of the input commands will be at the end of this section.

`wildcodes` contains a script called `WILDLINES`. This is a companion to `sfit`, which will open a graph of the generated spectrum, and a notepad of the `*.SFIT` input file for editing. This is done by starting with a folder containing a line list, a spectrum (in two-column format), and a `*.sfit` input file. Navigate to that folder and run `WILDLINES`, and follow the directions it gives. An example can be found in the `wildcodes` repo on github.

2.4. condor

If you're working with Simon, you may have access to the m15 and m45 multiprocessor servers for synthesising model grids. This has a slightly different format than normal, and needs some basic knowledge of bash scripting. Two examples are in the appendix, which generate a grid of temperature and gravities, synthesise models for each point on the grid, and generate spectra from these models. Refer to the short scripts, and adapt them for your custom grids.

The format for submitting a condor job comes in the form of a plaintext file, containing the arguments needed for processing. This is in the following form:

```
executable = $PATH_TO_EXECUTABLE
universe = vanilla
arguments = $ARG0 $ARG1 $ARG2 $ARGn
output = $OUTPUT_FILE
error = $ERROR_FILE
log = $LOG_FILE
queue
```

Here, the executable is the binary that we want to run, with the arguments passed with \$arguments. the output, error, and log files must also exist before the job is run, and the queue command at the end appends this job to the **condor** queue. NOTE: all file paths must be absolute paths, since condor has to unambiguously find all the files.

This is submitted to condor with the command `CONDOR_SUBMIT $FILE`. To see what jobs are in the condor queue, you can run the command `CONDOR_Q` to print a list. To remove a job from the queue (if you make a mistake or something), use `CONDOR_RM $JOB`. It is also worth mentioning that on m15, the binaries are not called **sfit**, **sterne**, or **spectrum**, but are batch versions of the code. Ask Simon (csj@arm.ac.uk) for more details.

3

Basic Assumptions

Author: Natalie Behara. Adapted from [Behara & Jeffery \(2007\)](#).

The radiative transfer codes STERNE, SPECTRUM, FFIT and SFIT, provide us with the necessary tools to analyze stellar spectra. These programs are designed and used for the study of evolved stars, such as helium-rich stars and chemically peculiar subdwarfs. Starting with either a high-resolution optical spectra or low-resolution spectrophotometry, this group of programs allows us to determine various physical quantities, such as the chemical composition, effective temperature, surface gravity, angular radius and the interstellar extinction. This chapter introduces the basic equations, focusing primarily on those used by STERNE and SPECTRUM, which were specifically designed to be suitable for the calculation of models of B-type stars with extreme compositions dominated by helium, carbon and nitrogen.

3.1. The SPECTRUM synthesis program

The LTE radiative transfer code SPECTRUM [Jeffery et al. \(2001\)](#) computes synthetic spectra, line profiles, equivalent widths, elemental abundances and curves of growth for individual lines. It was developed in Belfast by Dufton, Lennon & Conlon (unpublished), for the analysis of B star atmospheres. It has since been modified by [Jeffery & Heber \(1992\)](#) to include more detailed physics for computing the spectra of H-deficient stars. The modifications involve the use of better partition functions in the Saha equation (?) and the inclusion of scattering terms in the radiative transfer equation, which is solved using a Feautrier scheme. These modifications are necessary for the low densities and the scattering dominated continuous opacities encountered in the atmospheres of hydrogen-deficient stars.

SPECTRUM will read in model atmospheres computed by ATLAS or STERNE, and allows arbitrary and depth-dependent abundances. The continuous opacity sources follow those used in STERNE, either the ATLAS opacities, supplemented with tables for C I, C II, C III,

CIV, NI, NII, NIII and NIV ?, or the Opacity Project opacities. Given a model and a line list, SPECTRUM computes a synthetic spectrum over a large wavelength interval. The normalized spectrum, s_λ , is computed as a function of T_{eff} , $\log g$, microturbulent velocity, v_t , and chemical composition given as relative abundance by number n_i of species of i .

$$s_\lambda(T_{\text{eff}}, \log g, v_t, n_i, i = 1, \dots) = \frac{f_\lambda}{f_{\lambda c}} \quad (3.1)$$

The total emergent flux, f_λ , and the continuum flux $f_{\lambda c}$ may also be obtained.

The hydrogen line profiles are computed using broadening tables from [Lemke \(1997\)](#) and hence the broadening theory of [Vidal et al. \(1973\)](#). Neutral helium line profiles for HeI 4471, 4026, 4922 and 4388 Å are computed using broadening tables from [Barnard et al. \(1969, 1974, 1975\)](#), for HeI 4144 and 4009 Å using the broadening theory of ? and ?. The remainder of the HeI lines are computed using Voigt profiles or profiles from [Beauchamp et al. \(1997\)](#). Line profiles for ionized helium are computed from broadening tables by [Schöning & Butler \(1989\)](#). The metal line profiles are computed as Voigt functions, including Doppler, radiative and collisional broadening, as well as broadening due to microturbulence. Several databases of linelists are available for use with the program.

SPECTRUM also incorporates Opacity Project continuous opacities ([Seaton et al., 1994](#)) and depth-dependent compositions ([Behara & Jeffery, 2007](#)).

3.2. FFIT & SFIT

The Fortran90 program FFIT [Jeffery et al. \(2001\)](#) is used to determine the effective temperature, surface gravity, interstellar extinction (E_{B-V}), and angular diameter (θ) of stars by comparing spectral energy distributions. Using a grid of theoretical flux distributions, f_λ , we form the reddened flux distribution ϕ_λ :

$$\phi_\lambda(E_{B-V}, T_{\text{eff}}, \theta) = \theta^2 f_\lambda(T_{\text{eff}}) A_\lambda(E_{B-V}) \quad (3.2)$$

These are fitted to an observed flux distribution, F_λ , using a χ^2 minimization procedure, solving for one or all of the parameters.

The flux distributions are first resampled to the lower resolution of the theoretical fluxes. The specific extinction is taken from the average Galactic extinction law ?. The minimum in the multi-dimensional χ^2 surface is located using a downhill simplex method, implemented using a variant of the algorithm AMOEBA ?. In computing the statistic χ^2

$$\chi^2 = \sum_\lambda \frac{(F_\lambda - \phi_\lambda)^2}{\sigma_\lambda^2} \quad (3.3)$$

where σ_λ^2 are the variances of the binned fluxes, the errors associated with the best fit parameters x_i are given by the diagonal elements $(\alpha^{-1})_{ii}$ of the inverse of the covariance matrix α , whose elements are given by

$$\alpha_{ij} = \Sigma_\lambda \left(\frac{\delta\phi_\lambda}{\delta x_i} \frac{\delta\phi_\lambda}{\delta x_j} / \sigma_\lambda^2 \right) \quad (3.4)$$

At higher resolution, the spectrum of a star is defined primarily by its effective temperature, surface gravity and chemical composition. Using the program SFIT, and given a grid of high-resolution theoretical spectra, we can obtain an optimum fit in T_{eff} , $\log g$, and rotational velocity, $v \sin i$, of an observation by minimizing χ^2 , the weighted square residual between the normalized observed spectrum $S_\lambda = F_\lambda/F_c$ and the theoretical spectrum

$$s'_\lambda = s_\lambda(T_{\text{eff}}, \log g) \otimes I(\Delta\lambda) \otimes V(v \sin i, \beta) \quad (3.5)$$

where $I(\Delta\lambda)$ is the instrumental broadening and $V(v \sin i, \beta)$ is the rotational broadening.

In the computation of χ^2 , each wavelength point is assigned a weight, $w_\lambda = 1/\sigma_\lambda$. This is usually defined as the standard deviation about the mean flux in a line-free region of the observed spectrum, but may be given by some other means.

3.3. Validity of LTE Approximation

Departures from LTE occur when the radiative rates dominate over the collisional rates, which typically occurs at high temperatures and low densities. The departures will be largest where the opacity is high, such as in the cores of strong lines, since in this case the spectrum is formed high in the atmosphere where the density is low. Where LTE atmospheres are calculated using the Saha-Boltzmann equations, NLTE calculations require consideration of the detailed atomic processes for excitation and ionization, as expressed in the rate equations of statistical equilibrium.

The criteria for choosing LTE or NLTE is not simply a matter of effective temperature, as shown in Figure 3.1. The LTE approximation also starts to break down at low gravities. In this case, LTE models produce weaker line cores than NLTE models, which will have significant effects when fitting lines of very luminous helium stars, and may lead to errors in the estimated effective temperatures. NLTE atmospheres should be applied in the analysis of very hot stars, low density chromospheres, coronae of solar-type stars, and very cool stars in which electron densities are low.

In the blue-violet spectra of B stars, He line wings can be fitted using LTE models, however departures from LTE may be visible in some line cores. Departures become large for red or infrared lines, as these lines are not collisionally dominated, but rather are

Figure 3.1: Regions in $\log g$ vs. T_{eff} space where the LTE approximation is valid (?).

dominated by photoionization-recombination processes. The He I 6678 line in particular is much stronger in NLTE models than predicted by LTE models.

The stellar atmospheres created by `ltecodes` entirely assume the LTE approximation, and are designed primarily for stars with $T_{\text{eff}} \leq 35\,000$ K. It was shown that NLTE effects may be safely ignored for stars of this temperature by ?. A separate study by (Napiwotzki, 1997) showed that NLTE could only be ignored for stars with $T_{\text{eff}} \leq 30\,000$ K. However, his analysis was performed using LTE and NLTE models composed of only hydrogen and helium. In a recent analysis of two hydrogen-rich sdB stars, Przybilla et al. (2005) obtained temperature and gravity shifts of some 1200 K and 0.12 dex respectively by introducing opacity-sampled LTE model atmospheres and a non-LTE line formation code. Given Napiwotzki's result, the bulk of the difference would appear to be due to the improved opacity treatment.

3.4. The Microturbulent Velocity

In 1934, Struve and Elvey introduced a quantity called 'microturbulence' into the analysis of spectral lines ?. This quantity was used to reduce systematic errors in abundance analysis, a quantity that has become a regular parameter in stellar atmospheres modelling. Struve & Elvey supposed that the Doppler width for a line was much greater than due to thermal broadening alone. The additional width was attributed to a non-thermal motion in the stellar atmosphere, which they named microturbulence.

A satisfactory explanation to the nature of the motion responsible has not been achieved. The apparent extra broadening of the absorption lines is due to some kind of velocity field, however the characteristics of the field remain to be described. Some argue that micro-

turbulence is used in a completely arbitrary manner (?). The parameter ultimately serves to correct any deficiencies in model atmospheres, such as neglecting any departures from LTE, inhomogeneities, and errors in atomic data. For main sequence or near main sequence stars, it has been shown that microturbulence is necessary to reconcile the strengths of the saturated lines with the strengths of the weak lines ?. The accepted range of values for microturbulence in extreme helium stars is from 5 to 20 km/s, and for subdwarf B stars the range is from 0 to 5 km/s.

Derived abundances depend strongly on this parameter. Microturbulence, ξ , enters in the definition of the Doppler width:

$$\Delta\nu_D = \frac{\nu_i}{c} \left(\frac{2kT}{m_k} + \xi^2 \right)^{1/2} \quad (3.6)$$

where the frequency of the line centre is ν_i , the atomic mass of species k is m_k , k is the Boltzmann constant and T is the local temperature. In the case of purely thermal broadening (when ξ is neglected), the light atoms move faster than heavier atoms, since the speed is inversely proportional to the square roots of the atomic mass. Thus the lines of light atoms will be broader than the lines of heavier atoms. The microturbulent velocity effectively moves all atoms at the same speed, so it is possible to determine separately the kinetic temperature and the microturbulence.

In weak lines, increasing ξ broadens the line, but the equivalent width is conserved as the line becomes shallower. When a line is saturated, increasing ξ broadens the line but the depth remains the same, increasing the total absorption. An increase in ξ will thus increase the amount of backwarming in the atmosphere, and consequently raise the temperature in deeper layers.

4

sterne

4.1. History

The general problem of radiative transfer in stellar atmospheres in the limiting approximation of a plane-parallel semi-infinite stellar atmosphere in hydrostatic and local thermodynamic equilibrium has been treated extensively. While it is now common to consider departures from this approximation, there remain problems of considerable interest which need to be explored within it. The specific problem addressed here is that in which hydrogen is absent; this has important consequences for the way in which opacity is treated within a model atmosphere. Normally hydrogen is the dominant source of opacity in a stellar atmosphere; this has been an implicit assumption in the majority of treatments, e.g. ATLAS (Kurucz, 1970; ?). The absence of hydrogen, as encountered for example in extreme helium stars and R Coronae Borealis stars, places an increased onus on the accuracy and completeness of other opacity sources.

Very few codes for the calculation of stellar atmospheres have been written specifically to address this problem. The two principal examples are **sterne** Schönberner & Wolf (1974) and **marcs** Gustafsson et al. (1975). To compensate for the low hydrogen opacity, the original version of **sterne** considered in detail more sources of continuous opacity than other contemporary codes, particularly carbon and nitrogen. However, in the thirty years since **sterne** was first written, theoretical work has provided superior calculations of continuous opacities both for carbon, nitrogen and also for many other ions (Berrington, 1995). The contribution of absorption lines to the overall opacity has also seen major advances. Most model atmosphere codes now include a treatment of line opacity, either by the use of opacity distribution functions (ODF) (ATLAS6, Kurucz (1970)), opacity sampling (Peytremann, 1974); ATLAS12, (?) or complete line synthesis (Shulyak et al., 2004). While the ODF approach has since been implemented in **sterne** (Heber et al., 1984), the available ODFs use only $\approx 10^5$ lines and are restricted in composition.

In addition to improvements in opacity, many modern studies of stellar atmospheres

also consider departures from local thermodynamic equilibrium (non-LTE) (e.g. TLUSTY, Hubeny 1997, PRO2, Werner et al. 1997, PHOENIX, Hauschildt et al. ...). While departures from LTE are evident in the profiles of strong lines in stars of spectral types A and B, it remains the case that these are less important for the structure of the atmosphere as a whole than is a complete treatment of the continuous and line opacities (Przybilla et al., 2005). Moreover, since LTE models can be computed relatively cheaply compared with full non-LTE calculations, they are very important for exploring large volumes of parameter space.

The model atmosphere code **sterne**¹ assumes the stellar atmosphere can be approximated by a plane-parallel geometry and that it is in local thermodynamic, radiative and hydrostatic equilibrium (LTE). It had evolved in stages from a code developed to study planetary nebula central stars (?). ? subsequently applied **sterne** to the case of a pure helium atmosphere, pointing out the competition between pure electron scattering, which is grey and favours a shallow temperature gradient, and the contrast between high and low He I opacity above and below 504Å, which favours a steep temperature gradient. ? made minor changes to the code before Schönberner & Wolf (1974) introduced additional opacities. At this stage, the code considered opacities due to H, He, C, N and O photo-ionization and electron scattering, and was applied to the fine analysis of extremely hydrogen-deficient stars (Schönberner & Wolf, 1974) and to RCrB stars by Schönberner (1975). Heber & Schönberner (1981) added further continuous (bound-free) opacities and introduced line blocking from 52 He I lines and 400 UV metal lines via the synthetic spectrum approach. Other early applications of **sterne** to the analysis of extreme helium stars were presented by Walker & Schönberner (1981) and Heber (1983). ? (1984 or 1986 or a sig Ori E paper) introduced a capability to treat chemically stratified atmospheres. An ODF approach to incorporate line opacities was incorporated by (Heber et al. (1984) for hydrogen-rich compositions. Möller (1990) computed an ODF for a hydrogen-deficient mixture from the Kurucz & Peytremann (?) list of 265 000 lines.

Models computed with this H-deficient ODF were used in analyses of extreme helium stars by Jeffery & Heber (1992) and more than ten subsequent papers up to and including Pandey et al. (2006). Numerous minor improvements to the code were made between 1984 and 2001; the most recent descriptions were given by ? and Behara & Jeffery (2006).

¹The name **sterne** was attached to the code when it was submitted to the CCP7 program library in the mid 1980's (Jeffery Jeffery (1989)).

4.2. Radiative Transfer

The treatment of radiative transfer by both **sterne** and **spectrum** uses the Feautrier method described comprehensively by Mihalas (1978). The principal equations written out here provide a formal framework to describe the methods used in the computer programmes and other enhancements discussed thereafter.

If the source function is defined as

$$S_\nu = (\kappa_\nu B_\nu + \sigma_\nu J_\nu) / (\kappa_\nu + \sigma_\nu) \quad (4.1)$$

the standard transfer equation becomes

$$\mu \left(\frac{\partial I_{\mu\nu}}{\partial \tau_\nu} \right) = I_{\mu\nu} - S_\nu. \quad (4.2)$$

In the absence of scattering, $\sigma_\nu=0$ and J_ν can be calculated by quadrature from B_ν . Otherwise we must solve an integral equation for J_ν . Several methods have been proposed; we currently use that introduced by Feautrier (1966) in which the the transfer equation is written as a second-order differential equation subject to two-point boundary conditions.

In plane-parallel geometry, we consider the incoming and outgoing radiation at cosine angles $\pm\mu$;

$$\pm \mu \frac{\partial I_{z\pm\mu\nu}}{\partial z} = \chi_{z\nu} [S_{z\nu} - I_{z\pm\mu\nu}]. \quad (4.3)$$

Defining symmetric and asymmetric averages

$$u_\mu \equiv \frac{1}{2}[I_\mu + I_{-\mu}], \quad v_\mu \equiv \frac{1}{2}[I_\mu - I_{-\mu}] \quad (4.4)$$

and

$$d\tau_\nu \equiv -\chi_{z\nu} dz, \quad (4.5)$$

a single second-order equation for u may be obtained:

$$\mu^2 \left(\frac{\partial^2 u_{\mu\nu}}{\partial \tau_\nu^2} \right) = u_{\mu\nu} - S_\nu \quad (4.6)$$

with standard boundary conditions. We assume that the atmosphere is plane-parallel, static and symmetric in μ . Omitting the τ subscript, the source function may then take the form

$$S_\nu = \alpha_\nu \int \phi_{\nu'} J_{\nu'} d\nu' + \beta_\nu \quad (4.7)$$

where

$$J_\nu = \int I_{\mu\nu} d\mu \quad (4.8)$$

and ϕ_ν represents some redistribution function. Here, α represents the scattering coefficient.

Assuming complete redistribution and replacing integrals by quadrature sums, eqn 4.7 becomes

$$S_\nu = \alpha_\nu \sum_\mu I_{\mu\nu} + \beta_\nu \quad (4.9)$$

where β stands for the thermal term:

$$\alpha_\nu = \sigma_\nu / (\kappa_\nu + \sigma_\nu), \quad \beta_\nu = B_\nu \quad (4.10)$$

Replacing derivatives, eqn 4.6 can be rewritten as a standard second-order difference equation for each angle-frequency point and at $D-2$ depth points in the stellar atmosphere. These can be combined to form a matrix equation in \mathbf{u} which has a block tridiagonal structure and may be solved using an efficient forward-elimination and back-substitution procedure.

4.2.1. Radiative transfer in a slowly expanding atmosphere.

The standard Feautrier scheme assumes that velocity fields in the atmosphere are negligible. We have considered the case in which small vertical motions relative to the mean motion are present. An example is the atmosphere of a radially pulsating star. The most significant consequences are for the opacity, particularly the line opacity κ_l , which becomes angle-dependent

$$\kappa = \kappa_{\tau\mu\nu}. \quad (4.11)$$

If the depth-dependent velocity displacement is written as v_τ , then the total opacity may be written as,

$$\chi_{\tau\mu\nu} = \kappa_{c\tau\nu'} + \kappa_{l\tau\nu'} + \sigma_\tau, \quad (4.12)$$

$$\nu' = \nu \left(1 + \frac{v_\tau \mu}{c}\right), \quad (4.13)$$

since Thomson scattering is independent of frequency. In considering the line spectrum, this may be further simplified because the continuous opacity κ_c varies only slowly with frequency. Consequent ramifications can be accommodated entirely within the Feautrier scheme. The optical depth scales and scattering coefficients become angle dependent

$$d\tau_{\mu\nu} \equiv -\chi_{z\mu\nu} dz, \quad (4.14)$$

$$\alpha_{\mu\nu} = \sigma_\nu / (\kappa_{\mu\nu} + \sigma_\nu). \quad (4.15)$$

The final summation for the source function 4.9 must be written

$$S_\nu = \sum_\mu \alpha_{\mu\nu} I_{\mu\nu} + \beta_\nu. \quad (4.16)$$

Thereafter, evaluating the formal solution for the emergent fluxes and specific intensities must consider the angle-dependence of $\tau_{\mu\nu}$ so that

$$F_\nu = \int S_{\tau\nu} E_2(\tau) d\tau \quad (4.17)$$

$$I_{\mu\nu} = \int S_{\tau\nu} \exp\left(\frac{-\tau_\mu}{\mu}\right) d\tau_\mu. \quad (4.18)$$

Note that $S_{\tau\nu}$ is independent of μ . *The use of $E_2(\tau)$ may be inappropriate here*

4.3. Methods

The model atmosphere problem aims to provide a description of the outer layers of a star in terms of state variables temperature T and density ρ at a range of depth points broadly spanning the region where the continuum and absorption (or emission) lines are formed. Hence, a detailed model of the emergent spectrum may be computed by a formal solution of the radiative transfer equation over the wavelength range of interest.

sterne currently adopts a monochromatic optical depth grid $\tau_{\lambda=4000}$ with $D = 50$ unequally spaced points. The grid spacing is depth-dependent in order to allow fine spacing in the outermost layers and coarse spacing in deep layers.

Starting with a grey approximation to provide an initial description of T_τ , the equations of hydrostatic equilibrium are integrated using Runge-Kutta integration and Hamming's predictor-corrector method (Ralston & Wilf ?) to obtain ρ_τ .

The equation of state assumes a non-degenerate non-relativistic ideal gas. The electron density n_e is obtained by iteration of the ionization equilibrium for all atomic species included in the model.

The temperature must then be modified to obtain flux constancy through the atmosphere; this is carried out using the Unsöld-Lucy procedure (Lucy ?, Mihalas ?), recently modified Dreizler ?. However, the method requires a knowledge of the mean intensities J_ν throughout the model.

The source function is defined as

$$S_\nu = (\kappa_\nu B_\nu + \sigma_\nu J_\nu) / (\kappa_\nu + \sigma_\nu) \quad (4.19)$$

where B_ν is defined as the Planck function and κ_ν and σ_ν are the thermal absorption and scattering coefficients respectively. In the strict LTE approximation, $\sigma_\nu = 0$ and $S_\nu \simeq J_\nu \simeq B_\nu$. However, in hot stars and in hydrogen-deficient stars, electron scattering becomes a major opacity source, the strict LTE approximation breaks down and the standard radiative transfer equation

$$\mu \left(\frac{\partial I_{\nu\mu}}{\partial \tau_\nu} \right) = I_{\nu\mu} - S_\nu. \quad (4.20)$$

must be solved to obtain S_ν and J_ν . Here, $\mu \equiv \cos \theta$ is the angle between the direction of propagation of the radiation and the normal and $I_{\nu\mu}$ is the specific intensity in that direction. Originally, **sterne** solved Eq. 4.20 for S_ν using the method of Avrett & Loeser (?). Jeffery & Heber (?) obtained greater stability by introducing the method of Feautrier (?).

The abundances of all elements may be specified individually. They may also be scaled to the solar abundances, for which we have adopted the standard values as given by Grevesse & Sauval (?).

sterne assumes that all of the energy is transported radiatively, *i.e.* there is no convection. It also assumes that molecules do not contribute to either the equation of state or the opacity.

4.4. The **STERNE** model atmosphere code

The **STERNE** program calculates the structure of the stellar atmosphere. The structure is defined by the physical properties of the star, such as the effective temperature, surface gravity, chemical composition and microturbulent velocity. The effective temperature (T_{eff}) is defined as the temperature of a blackbody which emits the same amount of energy per unit area as the star. The surface gravity (g) is related to the mass (M) and the radius (R) of the star, and is given by,

$$g = \frac{GM}{R^2} \quad (4.21)$$

where G is the gravitational constant. The chemical composition defines the composition of the star's atmosphere, and may either be homogeneous throughout or vary with depth. The microturbulent velocity parameter is used to reduce systematic errors in the analysis of the chemical composition, and will be discussed in Section 3.4.

The code computes models by assuming plane-parallel geometry, hydrostatic, radiative, and local thermodynamic equilibrium (LTE). The choice of geometry reduces the atmospheres to a one-dimensional problem; all physical variables are represented as a function

of depth only. The assumption of LTE is equivalent to the assumption that collisional rates dominate over radiative rates. It allows the atmosphere to be characterized by one physical temperature at each depth. Microscopic processes are in detailed balance, and the densities of energy states are calculated from the Maxwell, Boltzmann and Saha relations. The validity of the LTE approximation is discussed in Section 3.3.

A static atmosphere allows us to ignore the subjects of pulsations and shocks, and any other time-dependent phenomena. With this assumption we make the further assumption of hydrostatic equilibrium. Outward pressure gradients exactly balance gravity. Dynamical effects are ignored. Hence, we assume that the atmosphere is not undergoing large-scale accelerations comparable to the surface gravity. The static gas pressure distribution just balances the gravitational forces, providing us with a mathematical relationship between pressure, P , and optical depth, τ ,

$$\frac{dP(\tau)}{d\tau} = \frac{\rho(\tau)g}{\kappa(\tau)} \quad (4.22)$$

where ρ is the density, g is the gravity and κ is the opacity. The optical depth is defined in relation to the geometric depth, z , as

$$\tau_\lambda = \int \kappa_\lambda dz \quad (4.23)$$

STERNE currently adopts a monochromatic optical depth grid $\tau_{\lambda=4000\text{\AA}}$ with $D = 50$ unequally spaced points. The grid spacing is depth-dependent in order to allow fine spacing in the outermost layers and coarse spacing in deep layers. The spacing of the optical depth points at which the solution is to be obtained is very important for the general overall accuracy of the calculation. Frequencies at which the atmosphere is optically thick will tend to carry less flux because the radiation can escape more readily at more transparent frequencies.

In a static atmosphere with a time-independent radiation field, the total energy absorbed by a given volume of material is equal to the energy emitted. This is the condition of radiative equilibrium; all the energy in the atmosphere is transported by radiation. In plane-parallel geometry this is equivalent to the condition that the flux, F , is constant throughout the atmosphere,

$$\sigma T_{\text{eff}}^4 = F = \int F_\lambda d\lambda \quad (4.24)$$

where σ is the Stefan-Boltzmann constant, and implies that the radiative flux is constant with height.

$$\frac{dF}{d\tau} = 0 \quad (4.25)$$

4.4.1. The Iterative Method

The process of model construction can essentially be separated into two parts. First, assume the atmospheric structure, and solve the radiative transfer equation. Then, having determined the radiation field, correct the atmospheric structure to ensure that the condition of radiative equilibrium (eqn. 4.24) is met. Using the corrected atmosphere, the process continues. The end result of this iterative process will be a self-consistent model, obtained by using the solution of the radiative transfer equation to generate the dependence of the temperature with depth in a manner that is consistent with radiative equilibrium.

The Grey Approximation

This method requires a starting approximation for the temperature distribution. In STERNE, the grey approximation is used, which assumes that the opacity is independent of wavelength. It provides a temperature distribution that scales with the effective temperature and is consistent with radiative equilibrium. The standard transfer equation in plane-parallel geometry is given by

$$\mu \left(\frac{\delta I_\lambda}{\delta \tau_\lambda} \right) = I_\lambda - S_\lambda \quad (4.26)$$

where I_λ is the specific intensity, μ is defined as $\cos \theta$, and θ is the angle between the direction of the ray and the normal to the surface. S_λ is the source function, and in a grey atmosphere with the condition of radiative equilibrium $S = J$, where J is the mean intensity. Equation 4.26 then reduces to

$$\mu \left(\frac{\delta I}{\delta \tau} \right) = I - J \quad (4.27)$$

which has the formal solution

$$J(\tau) = \frac{1}{2} \int_0^\infty J(t) E_1 |t - \tau| dt \quad (4.28)$$

and is known as Milne's equation. With the further assumption of LTE, $S_\lambda \equiv B_\lambda(T)$, and from the condition of radiative equilibrium, this implies that

$$J(\tau) = S(\tau) = B[T(\tau)] = \sigma T^4 / \pi \quad (4.29)$$

In the diffusion approximation, we find that at large optical depths

$$K(\tau) \approx \frac{1}{3}J(\tau) \quad (4.30)$$

where K is the second angular moment in the radiation field. In radiative equilibrium and plane-parallel geometry,

$$\frac{dK}{dz} = H \quad (4.31)$$

where H , the Eddington flux, is constant, and thus the solution of equation 4.31 is an exact integral

$$K(\tau) = H\tau + c = \frac{1}{4}F\tau + c \quad (4.32)$$

Since $K(\tau) \rightarrow \frac{1}{4}F\tau$ at large optical depths, it implies that at great depth

$$J(\tau) \rightarrow \frac{3}{4}F\tau \quad (\tau \gg 1) \quad (4.33)$$

$J(\tau)$ is expected to depart from this equation at the surface, as the optical depth decreases, which suggests the following expression for $J(\tau)$ (Mihalas 1978),

$$J(\tau) = \frac{3}{4}F[\tau + q(\tau)] = \frac{3}{4} \left(\frac{\sigma T_{\text{eff}}^4}{\pi} \right) [\tau + q(\tau)] \quad (4.34)$$

where $q(\tau)$ is the Hopf function. Combining equations 4.34 and 4.29 gives,

$$T^4(\tau) = \frac{3}{4}T_{\text{eff}}^4 [q(\tau) + \tau] \quad (4.35)$$

an equation for describing the temperature distribution. Using equation 4.28, the function $q(\tau)$ can be determined from the solution of the equation:

$$\tau + q(\tau) = \frac{1}{2} \int_0^\infty [t + q(\tau)] E_1 |t - \tau| dt \quad (4.36)$$

Values for $q(\tau)$ used in STERNE were obtained from Mark (1947).

Starting with equation 4.35, the process proceeds with the solution of the hydrostatic equation, which provides us with a description of the atmospheric pressure a function of depth (eqn. 4.22). In order to solve equation 4.22, we must first solve the equation of state. Starting with an initial estimate for the gas pressure, P_g , we solve for the electron pressure, P_e , for which we need the chemical composition. The electron pressure is obtained

by iteration of the ionization equilibrium for all atomic species ($Z = 1, 40$), including up to the 6th ionization stage. The partition functions are calculated using approximations due to Traving et al. (1966), Baschek et al. (1966) and Unsöld (1948). Using the estimate for P_g , and our value for P_e , it is now possible to calculate the opacity, κ . The detailed opacity calculations are outlined in Chapter 3. With the opacity quantity, we calculate a new estimate for P_g , and the iteration continues. Generally four iterations are sufficient for convergence.

The equation 4.22 can be solved in several ways. In STERNE, the numerical integration is initialized with a four point Runge-Kutta procedure. Once the first four points in the atmosphere have been solved, the integration is continued using Hamming’s predictor-corrector method (Ralston & Wilf 1960).

The next step in the model construction is to solve the transfer equation (4.26), by integrating the formal solution

$$F_\lambda = \int_0^\infty S_\lambda(\tau) e^{-\tau} d\tau \quad (4.37)$$

over optical depth. Originally, STERNE solved for S_λ using the method of ?. Jeffery & Heber (1992) obtained greater stability by introducing the method of ?. Although the Feautrier method proves to be an excellent technique in solving the transfer problem, some difficulties occur with the method at small optical depths. The implementation of Feautrier’s method in STERNE follows the method described by ?, who have developed a procedure that overcomes the difficulties in the upper atmosphere.

Once the radiation field is described, the temperature must be corrected to ensure that the condition of radiative equilibrium is met (eqn. 4.24). Departures from this condition form the basis for correcting the atmospheric temperature distribution. This correction is carried out using the Unsöld-Lucy procedure (??), recently modified to include new depth-dependent damping factors (?).

The iteration continues until the radiation field satisfies the desired conditions. The final result will be a description of model structure in terms of the optical depth at a given reference wavelength (τ_{4000}), including the temperature, gas pressure, electron pressure, opacity and a description of emergent flux as a function of wavelength.

In recent years, STERNE has been substantially modified to include a new treatment of the bound-free and bound-bound opacity and microscopic diffusion.

4.5. Opacity

The total monochromatic opacity is defined as

$$\chi_\nu = \kappa_\nu + \sigma_\nu \quad (4.38)$$

and the optical depth as

$$d\tau_\nu \equiv -\chi_\nu dz, \quad (4.39)$$

where z is geometric depth into the atmosphere. The thermal absorption coefficient κ_ν includes contributions from radiative bound-free (continuum) and bound-bound (line) transitions and is heavily dependent on atomic data, both empirical and theoretical. Here we describe how all of these data have been revised in **sterne**, using photo-ionization data from the Opacity Project (OP) (Seaton et al., 1994) and the IRON Project (IP) (?), and compilations of transition probabilities and other data from For completeness, we also describe the current treatment of the scattering coefficient.

4.5.1. Scattering

The scattering of light by free electrons is referred to as Thomson scattering, for which the classical formula

$$\sigma_e = (8\pi e^4/3m^2 c^4) = 6.65 \times 10^{-25} \text{cm}^2 \quad (4.40)$$

gives the cross-section *per electron* and is independent of frequency.

The scattering of radiation by bound systems, such as atoms and molecules, at frequencies much lower than the characteristic transition frequencies of the system, is known as Rayleigh scattering, σ_R . For frequencies $\nu \ll \nu_{ij}$ and characteristic resonant frequencies with strengths f_{ij} ,

$$\sigma_{\text{Rij}}(\nu) = \sigma_e f_{ij} \nu^4 / (\nu_{ij}^2 - \nu^2)^2. \quad (4.41)$$

Following Tarafdar & Vardya (?), this is computed from

$$\sigma_{\text{Rk}}(\lambda) = a_k / \lambda^4 (1 + b_k / \lambda^2 + c_k / \lambda^4) g_{0k} / u_k, \quad \lambda > \lambda_{\text{Rk}} \quad (4.42)$$

where a_k, b_k, c_k are given for each scatterer k (Table 4.1) with partition functions u_k and ground-state statistical weights g_{0k} for wavelengths greater than the characteristic wavelength, λ_{Rk} . Rayleigh scattering coefficients due to H, He, C, N, and O are included in **sterne**.

The total opacity per unit mass due to scattering is then given by

$$\sigma_\nu = \frac{N_A}{\mu_I} \left(\sigma_e + \sum_k \beta_k \sigma_{\text{Rk}}(\nu) \right) \quad (4.43)$$

where β_k corresponds to the fractional abundance of neutral ions of species k ($\sum_{jk} \beta_{jk} = 1$). N_A and μ_I refer to Avogadro's number and the mean atomic mass per atom respectively.

Table 4.1: Coefficients for Rayleigh scattering for H (?) and for He, C, N and O (Tarafdar & Vardya, 1969).

k	a_k	b_k	c_k	$\lambda_{\text{R}k}/\text{\AA}$
H	5.799×10^{-13}	2.452×10^6	4.801×10^{12}	1215
He	5.292×10^{-14}	0.470×10^6	0.182×10^{12}	584
C	4.288×10^{-12}	2.671×10^6	6.562×10^{12}	1657
N	2.319×10^{-12}	1.995×10^6	3.362×10^{12}	1200
O	7.585×10^{-13}	0.997×10^6	1.101×10^{12}	1302

4.5.2. Free-Free Absorption

For radiation at frequencies much closer to the characteristic frequencies, photons are scattered by free electrons passing near a bound system because of the creation of a transitory dipole moment. Cross sections for this process in hydrogen are given by

$$\alpha_{\text{ff}}(\nu, T) = \left(\frac{4e^6}{3ch} \right) \left(\frac{2\pi}{3km^3} \right)^{\frac{1}{2}} \frac{\overline{g_{\text{ff}}}(\nu, T)}{\nu^3 \sqrt{T}} \quad (4.44)$$

where $\overline{g_{\text{ff}}}$ is the thermal average of the Gaunt factor (Gingerich ?; Karzas & Latter ?)

$$\overline{g_{\text{ff}}}(\nu, T) \equiv \int_0^\infty g_{\text{ff}}(\nu, v) e^{-u} du \quad (4.45)$$

and $u \equiv (mv^2/2kT)$. Evaluating the constants we obtain,

$$\alpha_{\text{ff}}(\nu, T) = \frac{3.694 \times 10^8 \overline{g_{\text{ff}}}(\nu, T)}{\nu^3 \sqrt{T}} \quad (4.46)$$

If the free electrons are known to have a Maxwellian distribution, these calculations may be extended to include hydrogenic free-free absorption. Photoionization of multi-electron ions is decidedly non-hydrogenic. However, since very few experimental results are available, it is necessary to choose a theoretical approximation. Corrected for stimulated emission, the hydrogenic absorption cross-section per ion and per electron is,

$$\alpha_{\text{ff}}(\nu, T) = \frac{3.694 \times 10^8 \overline{g_{\text{ff}}}(\nu, T) Z^2}{\nu^3 \sqrt{T}} (1 - e^{-\frac{h\nu}{kT}}) \quad (4.47)$$

where Z is the atomic number of the species.

Table 4.2: Photoionization data included.

Opacity Project			
[1mm]	k	j	n_{ij}
H		I	55
He		I, II	13, 55
Li		I, II, III	25, 53, 55
Be		I, II, III, IV	55, 25, 54, 55
B		I, II, III, IV	55, 55, 26, 53
C		I, II, III, IV	50, 21, 38, 24
N		I, II, III, IV	36, 50, 32, 39
O		I, II, III, IV	50, 29, 25, 36
F		I, II, III, IV	50, 50, 50, 50
Ne		I, II, III, IV	50, 50, 50, 50
Na		I, II, III, IV	32, 50, 50, 50
Mg		I, II, III, IV	50, 32, 50, 50
Al		I, II, III, IV	41, 50, 31, 50
Si		I, II, III, IV	50, 51, 50, 31
S		I, II, III, IV	50, 50, 50, 50
Ar		I, II, III, IV	50, 50, 50, 50
Ca		I, II, III, IV	50, 17, 50, 50
Iron Project			
[1mm]	k	j	n_{ij}
Fe		I, II, III	50, 50, 50,

4.5.3. Bound-Free Absorption: Opacity Project Cross Sections

The absorption coefficient due to photoionization, or continuous opacity, represents the energy required to ionize an electron from a given bound state. Up to 2003 the bound-free opacities for H I, H⁻, He I, He II, He⁻, C⁻, O I, Mg I, Mg II, Al I, Si I, Si II, and Ca II were treated in **sterne** as in ATLAS (Kurucz ?). These were supplemented by additional tables for carbon and nitrogen, C I, C II, C III, N I, N II, and N III ((Peach, 1970)). The Kurucz and Peach bound-free absorption coefficients were calculated using a general formula for atomic photoionization cross sections together with estimated correction terms to the hydrogenic coefficient, calculated using exact Gaunt factors. Of these, only the opacities due to H⁻, He⁻ and C⁻ have been retained.

For photon energies below the ionization threshold, the cross-section is zero; for ener-

gies above the threshold, the cross-section is non-zero, decaying approximately as ν^{-3} for increasing ν . During the Opacity Project's (??) comprehensive re-derivation of photoionization and photoexcitation cross sections, it was discovered that photons with energies below the threshold could ionize the ion due to resonances with bound-bound transitions – known as photoexcitation of the core or PEC resonances, resulting in large deviations from the smooth hydrogenic functions. Any solution of the non-grey radiative transfer problem in stellar atmospheres should take these contributions to the opacity into consideration, as well as including the substantial improvement to the continuous opacity in well-behaved domains provided by the Opacity Project and other modern studies.

The Opacity Project computed monochromatic photoionization cross sections $\alpha_{ijk}(\nu)$ for each of the lowest-lying electron states i in H, He, Li, Be, B, C, N, O, F, Ne, Na, Mg, Al, Si, S, Ar, Ca and Fe where j denotes the ion species of the element k . These have been incorporated, with the exception of the iron cross sections, by computing the average contribution of each electron state within each wavelength interval 2Δ in the model atmosphere calculation

$$\bar{\alpha}_{ijk}(\lambda) = \frac{\int_{\lambda-\Delta}^{\lambda+\Delta} \alpha_{ijk}(\lambda') d\lambda'}{\int_{\lambda-\Delta}^{\lambda+\Delta} d\lambda'}. \quad (4.48)$$

These averages are computed on the model atmosphere wavelength grid from the tabulated cross sections at program initialization. The total cross section per atom is obtained by summing over electron state populations $\xi_{ijk}(\sum_i \xi_{ijk} = 1)$ and ion abundances β_{jk}

$$\alpha_{\text{bf}}(\lambda) = \sum_{ijk} \xi_{ijk} \beta_{jk} \bar{\alpha}_{ijk}(\lambda) \quad (4.49)$$

and transformed to give the total continuous absorption coefficient per gram κ from

$$\kappa_{\text{bf}}(\lambda) = \frac{N_{\text{A}}}{\mu_{\text{I}}} \alpha_{\text{bf}}(\lambda). \quad (4.50)$$

The way in which the OP data is included in the model atmosphere code is sufficiently general that any combination of ions may be selected, once the necessary cross sections have been downloaded from TOPbase (Cunto et al. ?). The ions currently included, together with the number of states treated for each ion (n_{ij}), are shown in Table 4.2.

Because OP cross-sections were calculate from theoretical model atoms in which the electron energy levels were up to 10% different from observed values, photoionisation edges do not always occur at the observed frequencies. In **sterne** we have tabulated the observed photoioniation edges separately and imposed a cutoff on the cross-section for photon energies below the threshold.

4.5.4. Bound-Free Absorption: IRON Project Cross Sections

Photoionization cross sections for the low ionization stages of iron were computed by the Opacity Project but have since been found to be of insufficient accuracy (Bautista ?). New calculations for Fe I, Fe II, Fe III, Fe IV and Fe V are being carried out by the Ohio State University group, in collaboration with the IRON Project. The new ground state Fe I cross sections are up to three orders of magnitude higher (Bautista & Pradhan ?), Fe II cross sections are up to an order of magnitude higher (Nahar & Pradhan ?), and Fe III cross sections are up to a factor or five lower (Nahar ?) than the OP data. These new cross sections for Fe I, II, and III have been incorporated into **sterne** using the same methods we employed for the OP cross sections.

4.5.5. Bound-Bound Absorption: Opacity Sampling

A major problem presented by the ODF approach is that hydrogen-deficient stars exhibit surfaces with highly-evolved chemical compositions and they can only be poorly characterised by a single mixture. Rather, they exhibit a range in average metallicity from 2 dex below solar to super-solar abundances, and large enhancements in carbon, nitrogen and oxygen. There are no two extreme helium stars with identical chemical compositions. Moreover, evolved stars show residual hydrogen abundances from normal down to less than 1 part per 10^4 .

An opacity sampling procedure has been implemented which accounts for contributions of up to 10^6 atomic lines. Whereas ODFs are only available for a few selected hydrogen-deficient mixtures, opacity sampling (OS) allows individual stellar abundances to be taken into consideration properly. As well, OS proves to be more flexible and adaptable than ODFs, as new values of oscillator strengths or new line lists can be easily incorporated without the need to recalculate extensive sets of opacity tables.

The opacity of a single line depends on the population of the absorber, the intrinsic strength of the transition – the oscillator strength or f -value, and the line profile. At frequency ν and optical depth τ , the opacity due to line i is represented by

$$\kappa_{\text{bb},i}(\nu, \tau) = \mathcal{N}_i(\tau) \cdot \alpha_{0_i}(\nu_i, \tau) \cdot \Phi(\nu - \nu_i, \tau) \quad (4.51)$$

where

$$\alpha_0(\nu_i, \tau) = \frac{\pi e^2}{m_e c} \frac{f}{\sqrt{\pi} \Delta \nu_D} \quad (4.52)$$

Defining v_0 as the frequency measured from line centre (ν_i) in units of Doppler half-width:

$$v_0(\tau) = |\nu - \nu_i| / \Delta \nu_D(\tau) \quad (4.53)$$

$$\Delta\nu_D(\tau) = \frac{\nu_i}{c} \left(\frac{2kT(\tau)}{m_k} + \xi^2 \right)^{1/2} \quad (4.54)$$

The atomic mass of species k is m_k and ξ the microturbulent velocity. For the line profile, we use the Voigt function,

$$\Phi(\nu - \nu_i, \tau) \equiv H(a(\tau), v_0(\tau)) \quad (4.55)$$

where $a(\tau)$ represents the scaled line-broadening coefficients. Omitting τ ,

$$a = \frac{\gamma_r + n_e \gamma_s + n_H \gamma_w}{4\pi \Delta\nu_D} \quad (4.56)$$

in which $\gamma_r, \gamma_s, \gamma_w$ are the radiative, Stark and Van der Waal's damping constants and n_e, n_H are the electron and hydrogen number densities, respectively.

The absorption coefficient per line and per absorber is then

$$\alpha(\nu) = \alpha_0 H(a, v_0) \quad (4.57)$$

Correcting the absorption for stimulated emission and multiplying by the number of absorbers in the lower state of the transition, we obtain the contribution from a given line

$$\begin{aligned} \alpha(\nu) &= \frac{\sqrt{\pi} e^2}{m_e c \Delta\nu_D} [1 - \exp(-h\nu/kT)] \\ &\times \exp(-\chi_L/kT) g_L f_{LU} H(a, v_0) \end{aligned} \quad (4.58)$$

where f_{LU} is the oscillator strength for a transition from a lower state L to upper state U , and χ_L, g_L are the excitation potential and statistical weight for the lower state. The total opacity at any selected frequency ν is then the sum of linear absorption coefficients due to all lines which have significant opacities at that frequency:

$$\begin{aligned} \alpha_{bb}(\nu) &= \frac{\pi^{1/2} e^2}{m c} [1 - \exp(-h\nu/kT)] \\ &\times \sum_{jk} \frac{\beta_{jk}}{G_{jk} \Delta\nu_{Dk}} \\ &\times \sum_L \exp(-\chi_L/kT) g_L f_{LU} \\ &\times H(a, v_0) \end{aligned} \quad (4.59)$$

Here the sum over L is the sum over all lines of ion j of atom k in a specified small frequency interval centered on ν , and the sum over jk is the sum over all ions j of all

atoms k . β_{jk} and G_{jk} represent the fractional abundances and partition functions of ion jk respectively. The subscript k in $\Delta\nu_{Dk}$ recognises that the Doppler half-width is a function of the contributing atom (m_k).

This summation must be carried out at every depth point and frequency point in the model atmosphere calculation, and many lines may contribute at each depth point. Consequently the implementation of the method in a computer code must be extremely efficient. We have devised a procedure, loosely based on Sneden et al. (?), which aims to minimize the number of cpu clock cycles by decomposing the various terms into depth dependent and frequency dependent quantities, as follows:

$$\nu'_L = \log(|\nu - \nu_L|) \quad (4.60)$$

$$\chi'_L = \chi_L \quad (4.61)$$

$$\phi'_L = \ln(g_L f_{LU}) \quad (4.62)$$

which only need to be established when reading in the linelist, providing that the reference frequencies ν used in the model calculation are specified. In addition, for ion j of atom k ,

$$\Delta\nu_{Dk} = \frac{\nu}{c} \left(\frac{2kT}{m_k} + \xi^2 \right)^{1/2} \quad (4.63)$$

$$\Delta'_k = \log(\Delta\nu_{Dk}) \quad (4.64)$$

$$\theta = 1/kT \quad (4.65)$$

$$\beta'_{jk} = \ln \left(\frac{\beta_{jk}}{G_{jk}/\Delta\nu_{Dk}} \right) \quad (4.66)$$

$$S' = \frac{\pi^{1/2} e^2}{mc} [1 - \exp(-h\nu/kT)] \quad (4.67)$$

are specified once for each frequency and depth point, but are independent of the line properties. To achieve this, we have introduced the approximation $\nu \approx \nu_i$ into (4.63) to improve efficiency. This is justified since lines are only considered to contribute to the local opacity if $|v|$ is smaller than some limit, *e.g.* 10^{-4} .

In the Doppler approximation, where radiative and collisional damping are neglected, we may write

$$H(a, v_0) \approx \exp(-v_0^2) \quad (4.68)$$

and the total line opacity can be computed very cheaply since equation 4.59 may then be written as:

$$\alpha_{bb}(\nu) = S' \sum_{Ljk} \exp(\beta'_{jk} + \phi'_L - \chi'_L \theta - \nu''_L \Delta''_k) \quad (4.69)$$

where

$$\nu_L'' = (\nu - \nu_L)^2 \quad (4.70)$$

$$\Delta_k'' = 1/(\Delta\nu_{Dk})^2 \quad (4.71)$$

The contribution of each line to the sum then requires only two multiplications, three additions and one exponentiation.

However simple tests with $a = 0.001$ show that the non-thermal contribution to the line profile is very important, especially in the ultraviolet. This can be dealt with, in a statistical approach, by tabulating the Voigt function or, rather, its logarithm, for carefully chosen values of a, v_0 :

$$H'_{pq} = \ln H(a_p, v_{0q}); \quad p = 0, n_p, \quad q = 0, n_q \quad (4.72)$$

Equation 4.59 may then be written

$$\alpha_{bb}(\nu) = S' \sum_{Ljk} \exp(\beta'_{jk} + \phi'_L - \chi'_L \theta + H'_{pq}) \quad (4.73)$$

where integers p, q are related to a, v_0 by:

$$\begin{aligned} p &= (\log(a) - p_0)n_p/\delta_p \\ q &= (\log(v_0) - q_0)n_q/\delta_q \end{aligned} \quad (4.74)$$

where $n_{p,q}, \delta_{p,q}, p_0, q_0$ are the number range and zero-point values for which H'_{pq} is tabulated. In practice, these indices will be evaluated from physical quantities by

$$\begin{aligned} p &= \text{nint} \left(\frac{n_p}{\delta_p} (\Gamma'_L + N'_d - \Delta'_k - p_0) \right) \\ q &= \text{nint} \left(\frac{n_q}{\delta_q} (\nu'_L - \Delta'_k - q_0) \right) \end{aligned} \quad (4.75)$$

where the damping constant Γ'_L is chosen from one of three approximations

$$\Gamma'_L = \log(\gamma_r/4\pi) \quad N'_d = 0 \quad (4.76)$$

$$\Gamma'_L = \log(\gamma_s/4\pi) \quad N'_d = \log(n_{ed}) \quad (4.77)$$

$$\Gamma'_L = \log(\gamma_w/4\pi) \quad N'_d = \log(n_{Hd}) \quad (4.78)$$

where $n_{...d}$ represents the appropriate particle density at depth point d and the γ 's refer to a particular line L . The choice of approximation must be made with care in order to

avoid unnecessary computation but without loss of accuracy. One example is the case of hot stars where Van der Waal's broadening (4.78) is negligible compared with electron broadening (4.77). For each line the maximum contribution for damping is selected. Having established α , the absorption coefficient per atom, we obtain the line-absorption coefficient per gram κ from

$$\kappa_{bb}(\nu) = \frac{N_A}{\mu_I} \alpha_{bb}(\nu). \quad (4.79)$$

Computed in this fashion, the opacity sampling method is able to account for the depth dependence of the variation with frequency of the line opacities. The method can also account for a change in composition simply by changing the model composition parameters.

4.5.6. Wavelength Grid and Line Selection

The wavelength grid may be adjusted to allow more or less structure in the opacity to be included. To treat the photo-ionization cross sections including the PEC resonances in detail, the grid should consist of a very high number of wavelength points. This would lead to unacceptable demands for computing time. In contrast, relatively few wavelength points are required to obtain smooth cross sections which exclude the detailed structure of the PEC resonances. Since such smoothing preserves the overall cross sections to within an error of 10%, we have chosen not to follow the PEC resonance structure in detail.

Similarly, including the opacity contribution from all absorption lines demands a large number of wavelength points. The wavelength grid must guarantee the selection of dominant lines in the photosphere and must also account for the contribution of weak lines in a statistically correct manner. If considering both atomic and molecular lines and 20 million lines or more need to be included, additional line selection at each grid point must be carried out to keep the number of lines within reason. However for hot stars, only atomic lines need to be accounted for. There are approximately 600 000 atomic lines in the Kurucz list (?). Therefore line selection is governed solely by the definition of the wavelength grid).

The grid used for the models presented in this paper allows a finer spacing at shorter wavelengths, increasing in coarseness with increasing wavelength. Just under 4 000 wavelength points are used, spaced by 0.5\AA at $\lambda < 900\text{\AA}$, 1.0\AA for $900 < \lambda < 3000\text{\AA}$, 2.5\AA for $3000 < \lambda < 9000\text{\AA}$, and at larger intervals thereafter.

The wavelength spacing was determined by demanding that the difference between one model and that computed with twice the number of grid points should be less than
????

In order to minimize the computational cost of producing OS models, the wavelength grid should become a function of effective temperature. Absorption lines to be included

would then be preselected using a starting approximation. Future versions of **sterne** will include an automatic grid selection based on the input parameters, and will be more uniformly spaced in frequency, rather than wavelength.

4.5.7. Specifying the composition

In practice, STERNE currently simplifies its input so that only carbon, nitrogen, oxygen, magnesium, aluminium, silicon, sulphur, calcium and iron are specified. Thereafter abundances for other species n_i are scaled according to:

$$3 \leq i \leq 5 : n_i/n_{12} = \alpha n_i/n_{12}|_{\odot}$$

$$9 \leq i \leq 12 : n_i/n_{12} \propto n_i/n_{12}|_{\odot}$$

$$15 \leq i \leq 16 : n_i/n_{16} \propto n_i/n_{16}|_{\odot}$$

$$17 \leq i \leq 25 : n_i/n_{20} \propto n_i/n_{20}|_{\odot}$$

$$26 \leq i : n_i/n_{26} \propto n_i/n_{26}|_{\odot}$$

5

spectrum

The formal solution code **spectrum** was written originally by Prof P.L.Dufton and extended by Drs D.J.Lennon and E.S.Conlon at Queen's University Belfast. It was adapted for use with H-deficient mixtures and considerably extended by one of us (CSJ). From a given model atmosphere and a line list including gf -values, radiative and collisional broadening constants and excitation energies, SPECTRUM can now compute synthetic spectra over large wavelength intervals and for many absorption lines. The usual output product is the normalized spectrum

$$s_\lambda(T_{\text{eff}}, \log g, v_t, n_i, i = 1, \dots) = \frac{f_\lambda}{f_c} \quad (5.1)$$

computed as a function of T_{eff} , $\log g$, microturbulent velocity v_t , and chemical composition given as the relative abundance by number n_i of species i . In addition, the total emergent flux f_λ , the continuum flux $f_{\lambda c}$ and specific intensities $I_{\lambda\mu}$ may also be obtained explicitly.

5.1. Formal Solution

For a plane-parallel stellar atmosphere, the emergent flux at frequency ν is defined by the standard integral over angle $\mu = \cos \theta$ of the specific intensity $I_{\nu\mu}$:

$$F_\nu = 2 \int_0^1 I_{\nu\mu} \mu d\mu \quad (5.2)$$

The specific intensity is obtained from the integral of the source function

$$I_{\nu\mu} = \int_\infty^0 S_{\tau\nu} \exp(-\tau/\mu) d\tau \quad (5.3)$$

over optical depth τ .

In the case of an atmosphere moving with uniform velocity $v = -\dot{r}^1$, it is sufficient to treat $S_{\tau\nu}$ as independent of μ . The integral over angle (Eqn. 5.2) needs only to consider the projected specific intensity by introducing the appropriate τ -independent frequency shift

$$\nu_{\mu} = \nu_0 \left(1 - \frac{v \cdot \mu}{c}\right). \quad (5.4)$$

Eqns. 5.2 – 5.4 are then sufficient to reproduce the line profile through the bulk of the pulsation cycle (cf. ?).

However, if radial velocity is a function of optical depth $v(\tau)$ (Fig. ??), then

$$\nu_{\tau\mu} = \nu_0 \left(1 - \frac{v(\tau) \cdot \mu}{c}\right) \quad (5.5)$$

and Eqn. 5.3 must treat the frequency dependence of S explicitly. The source function is conventionally defined by

$$S_{\tau\nu} = (\kappa_{\tau\nu} B_{\tau\nu} + \sigma_{\tau} J_{\tau\nu}) / (\kappa_{\tau\nu} + \sigma_{\tau}) \quad (5.6)$$

where $B_{\tau\nu}$ is the Planck function, the mean intensity $J_{\tau\nu}$ is found by solution of the transfer equation, the scattering coefficient σ_{τ} is normally independent of frequency, and the total absorption coefficient κ is the sum of the continuous absorption coefficient κ_c , which varies slowly with ν and the line absorption coefficient κ_l . Note that here κ is independent of μ .

In the case that $v(\tau)$ varies with depth, the specific intensities must be computed by integrating Eqn. 5.3 with

$$S_{\tau\nu\mu} = (\kappa_{\tau\nu\mu} B_{\tau\nu} + \sigma_{\nu} J_{\tau\nu}) / (\kappa_{\tau\nu\mu} + \sigma_{\nu}) \quad (5.7)$$

now calculated from the correctly projected local line opacity

$$\kappa_{l\tau\mu}(\nu) = \kappa_{l\tau\mu}(\nu_0 \cdot (1 - \frac{v(\tau) \cdot \mu}{c})) \quad (5.8)$$

These equations have been implemented within the LTE formal solution code SPECTRUM (?), which computes synthetic spectra and line profiles for a pre-computed model atmosphere structure. To the description of temperature and pressure as a function of optical depth provided by conventional model atmospheres, we add a description of the vertical velocity structure $v(\tau)$. Note that since τ increases with depth into the atmosphere, $v(\tau) > 0$ corresponds to a contracting layer and hence blue-shifted absorption as

¹In theoretical work, surface velocity conventionally follows the sign of the radial displacement vector. The minus sign arises here because we express the local velocity as a function of optical depth, which has the opposite sense to radius.

seen by a distant observer. $v(\tau) < 0$ corresponds to an expansion and red-shifted absorption. The plane-parallel approximation is justified because sphericity effects in the stars under investigation here are generally small, weakening the line but not influencing its shape.

In general, the input model atmosphere is one that has been computed elsewhere assuming hydrostatic, radiative and local thermal equilibrium. For the slowly varying phases of a star's pulsation cycle, these approximations are probably satisfactory except in the case of large amplitude pulsations in very luminous stars. In order to investigate departures from this approximation at phases close to radius minimum, we have introduced a prescription to raise or lower the local temperature $T(\tau)$ by an arbitrary amount at any point in the stellar atmosphere.

5.1.1. Computational Accuracy

Some numerical noise is introduced when very narrow perturbations are introduced into the model. The quadrature of Eqn. 5.3 is very sensitive to large perturbations in either κ_l (Eqn. 5.8) or $B_{\tau\nu}$. The reason lies primarily in the calculation of $I_{\nu\mu}$ at large μ , where the integrand in Eqn. 5.3 is very sharply peaked in τ .

A similar problem also arises when the velocity gradient in the atmosphere is large and the calculation involves narrow (unsaturated) lines. This is due to the line being shifted so far in neighbouring layers that the line source function is not adequately sampled by the quadrature over μ .

It was found that both problems could usually (but not always) be solved by a) increasing the number of optical depth points used in the quadrature of Eqn. 5.2 from 25 to 100 and b) increasing the number of quadrature points used to evaluate Eqn. 5.3. Typically, 10 points were used, compared with the customary 3 or 5 used for static atmospheres.

5.2. Line Profiles

Metal line profiles are computed as Voigt functions, including thermal and Doppler broadening due to microturbulence, and radiative and collisional broadening. Hydrogen lines are computed using broadening tables from Lemke (1997) and based on broadening theory by Vidal, Cooper & Smith (1973). Neutral helium line profiles for HeI 4471, 4026, 4922 and 4388Å are computed from broadening tables by Barnard et al. (1969, 1974, 1975). Profiles for HeI 4144 and 4009Å are computed from broadening theory by ? (1969) and by ? (1984), whilst the remainder are computed as Voigt profiles. Line profiles for ionized helium are computed from broadening tables by Schöning & Butler (1989).

6

Atomic Data

6.1. Hydrogen Lines

6.2. Helium Lines

The accurate modelling of neutral helium line profiles in stellar spectra is crucial to a wide range of astrophysical problems. Measuring the helium abundances in early-type main-sequence stars bears on star formation and galactic nucleosynthesis models, galactic structure and evolution and cosmological abundance measurements. Helium abundances in early-type subdwarfs provide diagnostics of stellar evolution and surface mixing due to convective and diffusive processes. Helium-line profiles are crucial for measuring surface gravities and effective temperatures in DB white dwarfs and in the luminous extreme helium stars, both highly evolved stars with uncertain evolutionary origins.

In turn, the accurate measurement of surface gravities and helium abundances is vital for understanding the properties of many types of star, particularly highly evolved stars. Therefore it is important that the basic physics assumed in making these measurements is satisfactory.

This report describes the treatments of neutral helium lines currently adopted in the spectral synthesis code SPECTRUM, an LTE package developed for the study of early-type stellar atmospheres by Dufton and coworkers (Lennon, Conlon, Rolleston) at the Queen's University Belfast, and by Jeffery at the Armagh Observatory. These methods are typical of those used in most commonly used astronomical spectral synthesis packages. It assesses whether these are sufficiently accurate for use in detailed astrophysical modelling. . . .

This paper does not go over the fundamental theory of line formation in neutral helium; this has been amply treated elsewhere.

6.3. Neutral Helium

Transitions in the neutral helium atom occur between levels that are strongly perturbed by electrons and other ions with the consequence that, at high densities, electron states are shifted and mixed and simple line broadening theories become inappropriate. This has been recognised over many years, and considerable experimental and theoretical effort has been directed towards understanding the detailed behaviour of the helium atom and its spectral properties.

Review major steps.... Griem, Gieske & Griem, Dufton, Barnard et al., Dimitrijevic & Sahal Brechot, Beauchamp et al.,

As a result, a number of approaches may be taken to modelling specific neutral helium lines in particular temperature and density regimes and due to different perturbers. However, in addressing the analysis of stellar atmospheres, a spectral synthesis code is often asked to treat several domains of parameter space at the same time. Increasing spectral resolution and signal-to-noise and new wavelength regions make tougher demands on the theoretical models. Consequently, atomic data from the best theoretical models are rarely available for the line, density and temperature required. Therefore a range of different approximations and models have to be adopted within a spectral synthesis code.

6.3.1. Voigt profiles

In its simplest form the normalised line opacity is given by

$$\kappa(\lambda, T, n_e, i) = gf_i s(\lambda, T, n_e, i) \quad (6.1)$$

where λ is the displacement from line centre, T is temperature, n_e is electron density, and i is a label identifying the transition with wavelength λ_0 . gf_i is the oscillator strength and s is a broadening function.

In the classical case for a singlet line, s may be approximated by the Voigt function

$$s = H(a, v)/D \quad (6.2)$$

where $a = n_e \Gamma_e / D$, $v = |\lambda| / D$, Γ_e is the electron damping width and D is the Doppler width containing thermal and dynamical components

$$D = \lambda_0 (2kT/mc + (v_t/c)^2)^{1/2}. \quad (6.3)$$

where v_t is the microturbulent velocity, k is the Boltzmann constant, c is the speed of light, and m is the mass of the parent ion.

6.3.2. Oscillator strengths for He I

6.3.3. Triplet splitting

The simplest extension to the standard Voigt function is to consider the splitting of triplet lines. Members of the triplet series split, under LS coupling theory, in the ratio 5:3:1. The two weaker components are separated from the principal component by amounts δ_1 , δ_2 . The resulting profile can be constructed applying the same electron width to all three components to obtain:

$$9s = 5H(a, v)/D + 3H(a, v_1)/D + H(a, v_2)/D \quad (6.4)$$

where $v_m = |\lambda - \delta_m|/D$.

How are $\delta_{1,2}$ computed?

6.3.4. Correction for ion collisions

A second refinement is obtained by correcting the electron width by a factor c_{ion} to allow for ion collisions:

$$\Gamma'_e = \Gamma_e(1 + c_{\text{ion}}) \quad (6.5)$$

Correction factors are given for selected lines by Griem et al. (1962) as:

$$c_{\text{ion}} = 1.36\alpha^{8/9}\sigma^{-1/3} \quad (6.6)$$

where α and σ both depend on the electron density, but the product $\alpha^{8/9}\sigma^{-1/3}$ does not. The convolved Voigt function profile for singlet and triplet lines is encapsulated in the SPECTRUM subroutine HEIVOIGT.

6.3.5. Ion broadening

Additional ion broadening in the line wings may be treated in an approximation that is phased in between $|\lambda| = 2D$ and $|\lambda| = S_i n_e^{2/3}$ so that in the full contribution,

$$s' = s \times R_i n_e / |\lambda|^{5/2}. \quad (6.7)$$

S_i and R_i are required.

Table 6.1: Atomic data require for semi-analytic treatment of He I line profiles

λ^0	rest wavelength of principal component of transition
gf	oscillator strength times lower level statistical weight
E	lower level excitation potential
Γ_e	electron damping constant
δ_1	separation of secondary from principal component in triplet
δ_2	separation of tertiary from principal component in triplet
c_{ion}	correction to Γ_e for ions
S	wavelength start value for ion broadening
R	constant for ion broadening
δ_F	separation of forbidden component from parent 2P- n D line
n_Q	upper level quantum number
w_Q	

6.3.6. Forbidden components

... not yet fully implemented ...

A final refinement may be applied when the contribution of an isolated forbidden component is to be included in the calculation of the line profile. Forbidden 2P- n P and 2P- n F components are found linked to both singlet and triplet 2P- n D transitions. Dufton showed that when they behave as isolated lines, the forbidden line oscillator strengths can be written in terms of the parent oscillator strength

$$gf_{Fi} = \alpha_{Fi} gf_i \quad (6.8)$$

where

$$\alpha_{Fi} = \frac{4\pi}{3} \left(\frac{h}{2\pi m_e} \frac{n_{Qi}^2 (n_{Qi}^2 - 4)}{w_{Qi}^2} \right)^{3/4} \quad (6.9)$$

The upper level quantum numbers, n_{Qi} and w_{Qi} are required for each 2P- n P and 2P- n F forbidden component, separated from their parent 2P- n D transitions by a wavelength δ_{Fi}

6.3.7. Data required

In order to model a given He I line profile in one or more of these approximations, the data shown in Table 6.1 are required (the subscript i is omitted in all cases).

Where available, these data are provided to SPECTRUM by the file `he1_lines.d`, a copy of which is given in the appendix. They are read in by subroutine `athe1`.

In practise, the number of lines for which any data other than λ^0 , gf , E and n_Q are available is limited, particularly in the ultraviolet, the infrared and towards the series limits. Consequently, the “default” option in the absence of a more sophisticated broadening theory is itself limited.

Where appropriate data do exist, these approximations are reasonably good in the low-density limit, *i.e.* for low-gravity stars, and for non-diffuse lines, *e.g.* the 2P– n S and 2S– n P series.

6.3.8. Semiclassical impact line widths

Application of data from Dimitrijevic & Sahal-Brechot 1990.

6.3.9. Electron broadening in the impact approximation

Barnard et al. (BCS) tables

6.3.10. Overlapping line theory

Beauchamp et al. (BWB) tables

Advantages and Drawbacks

The BCS tables have a number of drawbacks. The wavelength grid and range adopted for each density and line profile is different. This allows the narrower line cores to be correctly sampled at low density while including the far wings at high density. The far-wings can normally be treated satisfactorily in the $\lambda^{-5/2}$ approximation except where a forbidden component of a 2P– n D occurs (He I 4471 Å for example). Where the forbidden component is omitted from the low-density tables because of their reduced wavelength range, interpolation is impossible.

The BWB tables are much more extensive than the BCS tables, treating 21 lines in the blue compared with only four in the BCS tables. For modelling DB white dwarf spectra these are clearly the models to use.

At lower densities, this numerical advantage is less obvious since the classical approximations for isolated lines (see above) give profiles almost identical to the BWB tables. Moreover, the lower density limit of the BWB tables is 1 dex higher than that of the BCS tables for both 4921Å and 4471Å.

The BWB tables use a constant wavelength grid for each line, thus avoiding the omission of outlying forbidden components at low electron densities. However this is achieved at the expense of spectral resolution in the line core. This compromise may be appropriate for modelling white dwarf spectra, but for helium stars with $\log g < 5$, it is not satisfactory.

Ion dynamics effects, which are important typically within 1–2 Å from the line core, are neglected in the calculations. Therefore these tables are not necessarily appropriate where the line core is an important part of the line profile.

6.4. Ionized Helium

6.5. Metals: atomic data for stellar atmospheres

The passage of radiation through the atmosphere of a star is interrupted by numerous interactions, primarily with electrons. These electrons may be free or bound to an atom or ion. The result of a collision with a bound electron may be to liberate the electron altogether, or to excite the electron to a higher bound level within the ion. These three processes are sometimes referred to as scattering, photoionization or photoexcitation, and sometimes as free-free (ff), bound-free (bf) and bound-bound (bb) collisions.

The modelling of a stellar atmospheres (or any astrophysical object) and its emergent radiation requires a detailed model of how photons interact with electrons. Such processes can be approximately modelled if a relatively small number of basic quantities can be supplied, which carry information about the structure of the atom or ion being considered. These “atomic data” are fundamental to accurate astrophysical modelling. However, because these data are different for every transition in every atom and ion, and because there are billions of such transitions in nature, calculating, storing and curating these data for use are major problems in astrophysics.

In fact `spectrumis` is much more powerful than the B-star tag suggests. It may be used to model a wide variety of stellar spectra in LTE and HSE, providing they are warm enough not to contain molecules. Consequently, more extensive linelists may be required to construct useful synthetic spectra. There are many sources of atomic data; the following utilities enable these to be incorporated with existing QUB linelists.

Various databases exist and should be examined regularly for improvements. These include:

NIST

VALD

Kurucz

spectrum comes with a linelist optimized for early-B stars in the wavelength range 3800 - 5200 Å, with some additional lines, as well as more general linelists in the ultraviolet. A database for maintaining high-quality atomic data (**ltelines**) is described in the next chapter.

7

ltelines

For calculating model spectra of early-type helium stars in LTE, we maintain a database of atomic data for, mostly, blue-visual absorption lines of light elements. The data is sorted with one file for each ion. ¹

For each absorption line included, the database includes the wavelength, oscillator strength, radiative and collisional damping constants (where available), the excitation energy of the lower-level in the transition, the multiplet number (from Moore's revised multiplet tables). A reference for each of the oscillator strengths and damping constants are also given. The database is dynamic, with new lines being added as required. Some vetting is applied to ensure that only the most reliable data are included. Consequently the database is quite dynamic, with corrections and updates being included at arbitrary times.

A combined linelist can be constructed for use (eg) with SPECTRUM by executing the C-Shell program `LTE_LINE`. All the files necessary to run `lte_line` are available as a gzipped tar file. Usage should make reference to the original article describing this database (Jeffery C.S., 1991, Newsletter on 'Analysis of Astronomical Spectra', No. 16, p. 17), in addition to references to specific data sources. 2001 November

The linelists have been reformatted. Damping constants have been converted to natural gammas. Damping constants and oscillator strengths are now stored as logarithms. The conversion was carried out by Philip Dufton, QUB. Consequently the description by Jeffery (1991) is partially out of date as it refers to the units and format of the data.

A number of utilities used to convert various linelist formats have been developed over the years. These are provided here "as is" with no guarantees. Information File HTML Contents "read.me" file containing original ascii text for WWW pages Description of format and contents of ion files File to insert and mark the end of a linelist List of references to atomic data stored in ion files gzipped tar file Linelists for individual ions

¹An article describing the database originally appeared in the CCP7 newsletter (Jeffery C.S., 1991, Newsletter on 'Analysis of Astronomical Spectra', No. 16, p. 17). An archive version of the database may be found on the CCP7 website.

Table 7.1:

Ion	Sym	Z	I=0	II=+	III=++	IV=+++
Helium	He	2	367	2		
Lithium	Li	3	2			
Carbon	C	6	15	60	27	10
Nitrogen	N	7		220	23	
Oxygen	O	8	6	262	6	
Neon	Ne	10	17	33		
Magnesium	Mg	12		12		
Aluminium	Al	13		10	18	
Silicon	Si	14	1	19	26	14
Phosphor	P	15		24	6	1
Sulphur	S	16		88	32	
Chlorine	Cl	19		33		
Argon	A	20		96		
Calcium	Ca	22		21		
Titanium	Ti			45		
Chromium	Cr			5		
Iron	Fe	26	101	59	12	
Nickel	Ni					
Vanadium	V					

The number of lines in each file is given for each ion in Table 7.1

7.1. Major sources

* Linelists compiled by the Queens University of Belfast Hot Star group

* Linelists provided in the code of Uli Heber, atomic data is published for some of these lines by Heber 1983, AA 118,39, with references. Not all of the references have been entered. Much of the data is very old.

* A compilation by Kilian et al (1990), preprint - Munich. This compilation selectively lists data for lines with B star equivalent widths predicted to be greater than 10 mÅ, so is not complete for all multiplets, and only for wavelengths 4050 - 5060 Angstroms.

* Oscillator strengths from the Opacity Project.

* Where data have been essential for synthesizing B star spectra, additional lines have been extracted from Kurucz' linelists.

7.2. Programs

LTE_LINE: C-shell script to construct a composite linelist given specified ions (a web-based version of this script was available).

LTE_CONV: A Fortran utility to convert old linelist to new format. It will work on both complete line lists (including the atomic data at the start and references at the end) or raw ion files (such as Ni2.d).

VALD_QUB: A Fortran utility to convert line lists downloaded from the Vienna Atomic Line Database into the new QUB format.

synspec_qub: A Fortran utility to convert line lists in SYNSPEC format into the new QUB format.

LTE_SELECT: A Fortran utility to manipulate QUB-format line lists. It starts by reading in an optional initial linelist (QUB format) which will not be changed. An additional linelist (QUB format) is read in, it may be in the form of a Hubeny list, sorted by wavelength, or in some other order. Individual lines may be selected using various criteria including one or more of the following: wavelength region ions oscillator strength.

Examples of use: 1. Starting with an assessed list (such as created by "lte_line"), add additional lines from large database (eg Kurucz & Petrymann) 2. Starting with a large database (eg Kurucz & Petrymann) build up a reduced list ion by ion.

7.3. Individual line data for ltelines

The linelist format used by the Belfast line formation code SPECTRUM is a convenient means of storing atomic data needed for LTE line formation calculations. A substantial amount of data of varying quality is available in the literature. This database aims to maintain 'recommended' values for various atomic data, alongside information on sources, in a uniform manner. It does not necessarily contain the 'best' data, although this is a long term aim.

Atomic data for transitions in specific ions are stored in individual files (e.g. He1.d, C1.d, C2.d,). The individual line data include atom and ion identifiers, wavelength, oscillator strength, electron and radiative damping constants, excitation potential of the lower level in a transition, a multiplet identifier, and reference codes. The data are currently given in the following format.

Atom wavelength log electron radiative van der exc. multiplet references Ion (A) gf-value damping damping Waal's pot. (Moore)

```
0 0 0000.000 0.000 +00.000 +00.000 +00.000 0.000 00.00 OSC/EDAMP/RDAMP/VDW
```

Table 7.2:

Column	Explanation	Units	Example	
1	Atomic Number		6	Carbon
2	Ionisation stage		2	Singly ionised
3	Wavelength	Å	4267.2	
4	Oscillator strength	$\log gf$		
5	Electron damping width	$\log \Gamma_e$		
6	Radiative damping width	$\log \Gamma_r$		
7	van der Waal's damping width	$\log \Gamma_V$		
8	Excitation energy of lower level	eV		
9	Multiplet identification		48.00	
10	References for 4 – 7			

Notes

Where there is more than one entry for a given line, the recommended entry is entered normally. Other entries are preceded by a minus sign in the atomic identifier field. This is to preserve old data in the database.

Many damping constants are obtained from classical approximation formulae: these are indicated by a dash in the column for references. Where not even this level of sophistication is achieved, an approximate value may have been entered. No reference is cited, and fewer significant figures are placed in the table. A substantial effort is still required to extend the damping constant data.

8

idlines

An IDL procedure to display a region of spectrum, optionally with a model superimposed on the observations, together with the positions of selected lines. Positions of lines in common atomic spectra are marked in the lower panel in logarithmic form. Lines of selected atoms are identified against the observed spectrum and fit.

This doc refers to a much older version ... update to 2019.

Include examples of recent plots

8.1. Usage

IDL> idlines, *specfile*, *linelist*, *xlo*, *xhi*, *xr*, *atoms*, [*thresh*, [*rv*], [*Keywords*]

8.2. Arguments

<specfile> - character string - name of file containing spectrum (and fit) assumed to be x,y file with 3-line header

<linelist> - character string - name of file containing eq.widths assumed to be 'spectrum' output

<xlo> - real variable - lower limit of plot

<xhi> - real variable - upper limit of plot

<xr> - real variable - xrange to show in each panel of plot

<atoms> - integer vector - atomic numbers of spectra to be identified

<thresh> - real variable - threshold eq width to identify lines (Angstrom)

<rv> - real variable - radial velocity of spectrum (km/s) (Use this to match line-ids to observed positions).

8.3. Keywords

/FIT - overplot the fit
 /EW - read and select the lines using equivalent widths
 /NF - read and select the lines using $n*gf$ (central opacities)
 /ALL - plot individual atomic spectra schematically
 /MULT - add multiplet labels to line ids
 /STIS - to allow for air/vacuum shift at 2000Å.
 /XTEND - extend line identification marks (useful in some cases)
 /XPAND - expand plot by factor of 5
 /DUPLEX - plot two regions of spectrum on the same panel (overridden by /ALL)
 /PRINT - plot hardcopy as a postscript file

Hint: To obtain a nice display

IDL> window,xsize=1024,ysize=600

8.4. Input Files

Spectra

sp2: single spectrum (could be observed or model)

sfit: observed spectrum and model fit sfit output file containing observation and solution.

Keyword /FIT must be specified

Linelists

lte_lines: These linelists contain no information about relative line strengths, but can be used for inspection of data independent of any models. Many of the linelists in this format contain information about Moore multiplet numbers, and these can be added to the plot using the keyword /MULT. The linelist is read in assuming this format by default – i.e. if neither keyword /NF or /EW is supplied.

/NF: $\langle linelist.used \rangle$ These linelists are generated by SPECTRUM immediately after a linelist and model atmosphere are read in. This type of linelist can also be read assuming default options. However, the final column contains the product of the lower level population * the gf-value at optical depth $\tau = 0.1$ – thus giving an approximate indication of the line strength (neglecting all line-broadening). This can be used to select the lines identified using a parameter thresh (see argument list). To do this, the keyword /NF must be supplied.

/EW: $\langle linelist.eqwid \rangle$ The function calc_lines in SPECTRUM produces a file containing equivalent widths for all lines in the atomica data input list, with user-specified abundances. The file format is significantly different from the above two formats, so cannot be read

unless the keyword /EW is also supplied (at present). The number of lines identified can be changed by adjusting the threshold parameter

8.5. Prologue

PRO idlines, specfile, linelist, xlo, xhi, xr, atoms, thresh, rv, *FIT = kft*, *EW = kew*, *NF = knf*, *ALL = kall*, *STIS = kst*, *PRINT = kpr*, XTEND = kxt, XPAND = kxp, MULT = kmlt, DUPLEX = kdup

```

;-----
;
; idlines
;
; IDL procedure to display
; a) a region of spectrum, together with a fit, if supplied,
; b) positions and relative strengths (gf or W_lambda) of lines in
; common atomic spectra may be marked in the lower panel.
; c) lines of selected atoms are identified in the top panel
;
; Command arguments:
;
; specfile - character string - name of file containing spectrum (and fit)
; assumed to be x,y file with 3-line header
; linelist - character string - name of file containing eq.widths
; assumed to be 'spectrum' output
; xlo - real variable - lower limit of plot
; xhi - real variable - upper limit of plot
; xr - real variable - range of individual plot
; atoms - integer vector - atomic numbers of spectra to be identified
; [ thresh - real variable - threshold eq width or line strength to identify
lines ]
; [ rv - real variable - radial velocity of spectrum ]
;
;-----

```


9

ffit

The method adopted here to measure effective temperature, angular diameter and interstellar extinction was to fit the reddened theoretical flux distribution

$$\phi_\lambda(E_{B-V}, T_{\text{eff}}, \theta) = \theta^2 f_\lambda(T_{\text{eff}}) A_\lambda(E_{B-V}) \quad (9.1)$$

to the observed flux distribution F_λ using the method of χ^2 minimization. The flux distributions are first resampled to the resolution of the theoretical flux distributions, this being lower. The specific extinction A_λ is taken from the average Galactic extinction law due to Seaton (1979). In computing

$$\chi^2 = \sum_\lambda \frac{(F_\lambda - \phi_\lambda)^2}{\sigma_\lambda^2}, \quad (9.2)$$

σ_λ^2 are the variances of the binned fluxes. The errors associated with the best fit parameters x_i are given by the diagonal elements $(\alpha^{-1})_{ii}$ of the inverse of the covariance matrix α , whose elements are given by

$$\alpha_{ij} = \sum_\lambda \left(\frac{\partial \phi_\lambda}{\partial x_i} \frac{\partial \phi_\lambda}{\partial x_j} / \sigma_\lambda^2 \right). \quad (9.3)$$

The minimum in the multi-dimensional χ^2 surface was located using the downhill simplex method (?), implemented using a variant of the algorithm AMOEBA (?). The method was proven to give identical results to an independently developed brute-force algorithm (cf. ?). The principal difference between our version of AMOEBA and that published by Press et al. is that ours passes both the free parameters and the observed spectrum to the function to be minimized. In this case, the function is χ^2 (cf. **chisq**, ?).

In applying **ffit**, care should be taken to ensure that the normalization of theoretical and observed fluxes are carried out at optical wavelengths (for example), otherwise small errors in E_{B-V} and T_{eff} can lead to major errors in θ . Although E_{B-V} may be found as an

independent parameter in each fit, the final results should be constrained to have a single “average” value of E_{B-V} for repeated observations.

ffit was tested by application to a spectrum of Vega used for calibration of the *Hubble Space Telescope* (Colina et al. 1996). The calibration spectrum was restricted to match the IUE wavelength interval, and supplemented with UBVRI photometry, assuming $U = B = V = R = I = 0.0$. The photometry was converted to flux units with the calibration constants $C_\lambda = -20.94, -20.51, -21.12, -21.89, -22.70$, respectively. Using a grid of ATLAS9 model atmospheres (?) with $\log g = 4.0$ and $[\text{Fe}/\text{H}] = -0.5$, **ffit** yielded $T_{\text{eff}} = 9617 \pm 24\text{K}$, $\theta = 7.67 \pm 0.02 \cdot 10^{-9}$ radians and $E_{B-V} = 0.000 \pm 0.004$ (formal errors). Both T_{eff} and θ differ by less than 1% from the result reported by ? (1994).

10

sfit

Our goal was to estimate the various parameters of the stellar atmosphere (effective temperature, surface gravity, chemical composition, etc.) by finding the combination that produces a theoretical spectrum which most closely resembles the observed spectrum.

In addition to the natural broadening of spectral lines in the stellar atmosphere by processes described above, additional broadening processes must be considered. These processes are applied to the synthetic spectra before comparison with the observed spectrum and include:

- *Instrumental broadening* $I(\Delta\lambda)$: each spectrum is convolved with a Gaussian having a FWHM $\Delta\lambda$ equal to the instrumental resolution measured from the comparison lamp emission lines and being 0.46\AA .
- *Rotation broadening* $V(v \sin i, \beta)$: each spectrum is convolved with the rotation broadening function (Unsöld 1955, Dufton 1972), assuming a limb darkening factor $\beta = 1.5$. The projected rotation velocity $v \sin i$ is a free parameter of the model.
- *Acceleration broadening* $A(\delta v)$: the change in radial velocity δv during each 100s exposure of V652 Her is typically 1 km s^{-1} and around minimum radius rises to $\sim 10 \text{ km s}^{-1}$. An experiment was performed in which each spectrum was convolved with a boxcar of full width equal to the acceleration. In practise, more consistent solutions were found without this broadening being applied.
- *Projection broadening* $P(v - \bar{v})$: the projection of the spherical expansion onto the line of sight convolved with the specific intensity of the emergent flux distorts and broadens the line profile as a function of phase, as discussed elsewhere (?). The asymmetries predicted for V652 Her, when convolved with other effects were found to be negligible. We have been unable to detect any asymmetry in the line profile as a continuous function of pulsation phase.

10.1. sfit: solve

For a given observation, an optimum fit in T_{eff} , $\log g$ and $v \sin i$ was obtained by minimizing χ^2 , the weighted square residual between the normalized observed spectrum $S_\lambda = F_\lambda/F_c$ and the theoretical spectrum

$$s'_\lambda = s_\lambda(T_{\text{eff}}, \log g) \otimes I(\Delta\lambda) \otimes V(v \sin i, \beta) \otimes A(\delta v) \otimes P(v - \bar{v}). \quad (10.1)$$

The model spectrum for arbitrary T_{eff} , $\log g$ was obtained using a two dimensional polynomial interpolation in the discrete model grid. For accuracy, the algorithm **polin2** (?) was adopted. The χ^2 -minimization was carried out using the new-variant algorithm **amoeba** described above. The method was proven to be robust by repeated applications using different model grid spacings and starting values.

In the construction of χ^2 , each wavelength point was given a weight $w_\lambda = 1/\sigma_\lambda$, defined as the standard deviation about the mean flux in line-free regions, where $\sigma_\lambda \sim 0.01$. Since the cores of strong HeI lines still consistently fail to provide agreement between theory and observation, they were partially excluded from the fit by assigning a lower weight to the corresponding wavelength points ($\sigma_\lambda = 0.1$).

In any such fitting procedure, the normalization of the observed spectrum can be of crucial importance (cf. ?). The initial normalization was carried out by fitting a high-order polynomial to apparent sections of “continuum”. The presence of even a few weak lines can mean that this procedure sets the “continuum” too low. We adopted a single improvement iteration (cf. ?). Having found a best-fit s'_λ , the ratio S_λ/s'_λ was trimmed to exclude values more than 5% from continuum and convolved with a low-pass Gaussian filter of FWHM 18Å. This provided a renormalization function for each spectrum which departed not more than 1% from unity, with a standard deviation of $\lesssim 0.5\%$. The renormalization had no effect on individual line profiles.

An extension of the above code allows for the variation of one other parameter, the helium abundance n_{He} for example, was not used in the current investigation but is noted for completeness. The grid of model atmospheres and synthetic spectra may be extended to three dimensions T_{eff} , $\log g$ and the fractional helium abundance n_{He} . Interpolation is carried out first in n_{He} to obtain a subgrid in which the two-dimensional interpolation for T_{eff} and $\log g$ can be carried out as above.

10.2. sfit: synth

If T_{eff} , $\log g$ and $v \sin i$ are known, the composition of a star may be obtained by adjusting the abundances of the different atomic species which contribute to the absorption spectrum,

together with the microturbulent velocity (v_t), so that the theoretical spectrum matches the observed spectrum. This can be achieved by minimizing the same weighted χ^2 residual between observed and theoretical spectrum as used by `sfit_tgv`. However, in the present case, the number of free parameters, namely the abundances of H, C, N, O, Al, Si, P, S, Ne, Mg, and Fe and v_t , was so large that precomputing multidimensional grids of theoretical spectra would have been prohibitive. The solution adopted was to compute synthetic spectra in real time as demanded by the χ^2 minimization procedure, `amoeba`. The same line-broadening (rotation, instrumental, acceleration, projection) could be introduced as before.

In principle, this code `sfit_synth` could solve simultaneously for as many parameters as are required. It was found to be more practical to restrict each run of the code to between two and four parameters. A single model atmosphere is assumed as input, so that T_{eff} , $\log g$ and $v \sin i$ remain fixed for a given solution. Then the code would attempt to solve for v_t and one chemical abundance together, or for two or three chemical abundances simultaneously, whilst other chemical abundances were kept fixed.

10.3. Operation of the Programs

Given the physical assumptions outlined above and either a high-resolution optical spectrum or low-resolution spectrophotometry covering ultraviolet and visual wavelengths (at least), these programs allow us to derive various physical quantities in an objective manner. The outputs are either T_{eff} , $\log g$, $v \sin i$, v_t and chemical composition from a high-resolution spectrum, or T_{eff} , θ and $E_{\text{B-V}}$ from spectrophotometry. A block diagram illustrating the procedures, inputs and outputs, is shown in Fig. 1. Note that it is essential to ensure that the composition used as input to the model atmospheres is consistent with that derived as output from the spectral analysis. The latter critically affects the background opacities and hence the temperature stratification in the former, especially where hydrogen is absent from the stellar atmosphere. Therefore a few iterations may be necessary before a final solution is achieved.

10.4. SFIT - some corrections – 2013

10.4.1. The fitting function

Call the observed flux F_λ . Assume that this is normalised to the local continuum to give a function A_λ . Note that F_λ is related to the surface flux emitted by the star $F_{\lambda,0}$, by

$$F_\lambda = F_{\lambda,0} \left(\frac{r}{d} \right)^2$$

where r is the stellar radius and d is the distance.

Call the theoretical flux f_λ , and the local continuum flux c_λ . The object of SFIT is to find the function

$$a_\lambda \equiv \frac{f_\lambda}{c_\lambda} = A_\lambda \quad (10.2)$$

For a single star, f_λ and c_λ are functions of many quantities including effective temperature T_{eff} , surface gravity g , composition, microturbulent velocity v_{turb} , radial velocity v_{rad} , projected rotation velocity $v_{\text{rot}} \sin i$, and so on. We will denote these “free parameters” by p .

For stability reasons, it is best if the numerical values of p are roughly of similar magnitude. Since we have to solve systems of linearized equations, which involves matrix inversion, it is best to avoid large magnitude differences amongst p . Hence we typically choose $T_{\text{eff}}/1000 \text{ K}$, $\log g$ (cgs), $\log r/r_1$, and various v 's in km s^{-1} , so that p is uniformly of order unity.

In the case of a binary star, the spectra of both components are combined. We denote the two components by subscripts 1 and 2. In addition to all of the above parameters being duplicated, it is necessary to take into account the *relative* contributions of the two components to the total flux, which is proportional to the *square* of their relative radii r_1, r_2 . Thus, dropping subscript λ , a must now be written,

$$a \equiv \frac{f}{c} = \frac{r_1^2 f_1 + r_2^2 f_2}{r_1^2 c_1 + r_2^2 c_2} \quad (10.3)$$

10.4.2. χ^2 minimisation and parameterisation

Since a is a multi-valued function and Eqn. 10.2 is extremely non-linear, a solution is generally sought by minimizing some statistic such as

$$\chi^2 = \sum_\lambda (A - a)^2$$

Various methods are available; the choice depends somewhat on the number of free parameters (a large number might suggest a Monte-Carlo or Genetic Algorithm approach) and whether the functions are differentiable or not. Differentiable functions permit a Newton-Raphson type approach such as the Levenburg-Marquardt method. Otherwise, brute-force searches such as the downhill simplex (AMOEBA) may be preferred.

In addition to finding an optimal set of parameters, it is desirable to know the uncertainty (or error) associated with each free parameter in the solution. This can be established from the leading-diagonal elements in the covariance matrix associated with the solution – essentially the derivative of a with respect to a given parameter p .

In SFIT, most of these derivatives are evaluated numerically. Thus to evaluate $\partial a/\partial p_i$, for example, we would in general compute a for p and $p + \delta p$ and evaluate

$$\frac{\partial a}{\partial p} = \frac{a(p + \delta p) - a(p)}{\delta p}$$

In the case of binary stars, we require the derivatives of the combined spectrum a (Eqn. 10.3) wrt to the parameters of each component separately, *e.g.*:

$$\frac{\partial a}{\partial p_1} = \frac{r_1^2}{c} \left(\frac{\partial f_1}{\partial p_1} - \frac{\partial c_1}{\partial p_1} \frac{f}{c} \right) \quad (10.4)$$

where f and c are implicit in Eqn. 10.3. The *exception* is $\partial a/\partial r_{1,2}$, in which case we obtain:

$$\frac{\partial a}{\partial r_1} = 2r_1 \frac{f_1 - (f/c) * c_1}{c} \quad (10.5)$$

10.4.3. Features and Bugs

However, during the evolution of SFIT to treat binary stars the parameter used to describe the relative radii has changed from r to $q = \log r$ (see above). There are two consequences to note.

1. The values of q_1 and q_2 reported in the SFIT output represent $\log r_1$ and $\log r_2$ in some arbitrary units. The relative radii of the two stars are given by

$$\frac{r_2}{r_1} = 10^{(q_2 - q_1)}$$

This is correctly documented on the SFIT webpages. *In the latest example you have $q_1 = 1.0$, $q_2 = 1.067$, hence $r_2/r_1 = 1.17$ - which seems fine to me.*

2. Through infrequent use, two problem have crept into the code with regard to the errors which SFIT reports as δq_1 and δq_2 . First, the coded form of Eqn. 10.5 omitted the factor $2r_1$. Second, Eqn. 10.5 should have been expressed for q rather than r :

$$\frac{\partial a}{\partial q_1} = \ln 10 \frac{2r_1^2}{c} \left(f_1 - \frac{c_1 f}{c} \right) \quad (10.6)$$

and similarly for $\partial a/\partial q_2$. *The omission of a factor of $\ln 10 \cdot 2r^2 \approx 6.30$ from this equation for the derivative suggests to me that the errors in q_2 reported by SFIT should be divided by at least this factor, implying $\delta q_2 \approx 0.4$.*

The relevant lines in `lte-codes-3.2.X/src/libraries/xfit/spec_tghv_bin.f90` should read:

```
! dA/d(Q1)
DERIVS(5) = 2*TAPM_LN10 * R1SQ * ( FINT1(NW,1) - F * CINT1(NW,1) ) / CNU
...
! dA/d(Q2)
DERIVS(11) = 2*TAPM_LN10 * R2SQ * ( FINT2(NW,1) - F * CINT2(NW,1) ) / CNU
```

11

Dynamical atmospheres

This draft chapter is based on early work with BW Vul and discusses methods for treating artificial temperature and velocity profiles in the model atmosphere. `spectrumnow` includes sophisticated tools for integrating with a dynamical pulsation model to compute realistic time-dependent spectra based on hydrodynamical models of a pulsating star.

11.1. Non-standard Line Profiles

An interesting problem arose in relation to the behaviour of various absorption lines through minimum radius of BW Vul (Fig. 7). A Kurucz model atmosphere with solar composition, effective temperature 24 000 K and surface gravity 3.5 dex (cgs units) was adopted as a reference model. This is close to values measured by [?], allowing for the range in T_{eff} around the pulsation cycle and our interest in phases around minimum radius, which corresponds to maximum temperature. A standard value of 5 km s^{-1} was adopted for the microturbulent velocity. Line broadening for the optical He I lines was obtained from the tables of [?].

11.1.1. Velocity Perturbations

The first hypothesis is that the line profiles observed in BW Vul can always be reproduced by introducing a non-uniform but physically plausible velocity field $v(\tau)$ in the stellar atmosphere.

Interesting velocity fields involve both infalling material and outflowing material, normally converging to an intermediate stationary point at a specified optical depth τ_0 (Fig. 11.1). The extent of the transition layer between infalling material with $\tau < \tau_{\text{inward}}$ and outflowing material with $\tau > \tau_{\text{outward}}$ has been parameterized using

$$\alpha = \tau_0 / \tau_{\text{inward}} = \tau_{\text{outward}} / \tau_0. \quad (11.1)$$

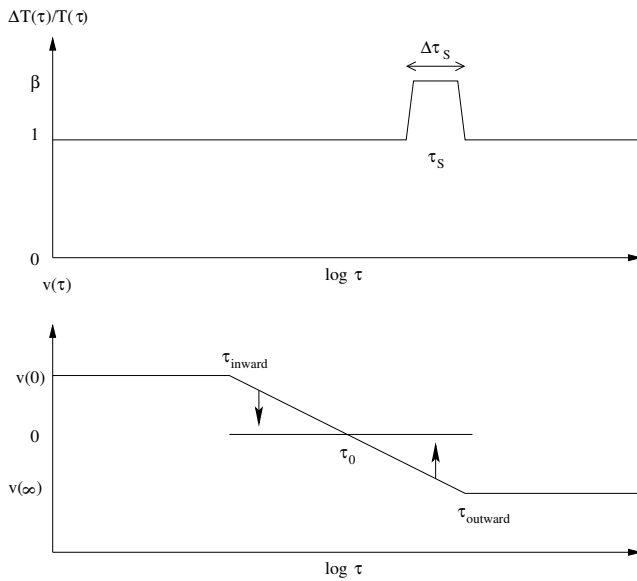


Figure 11.1: Diagram showing how a temperature perturbation (top) and a velocity field $v(\tau)$ (bottom) are introduced to the structure of the model atmosphere, indicating various quantities described in the text. In representing a pulsating star passing through minimum radius, the stationary point τ_0 is moving outwards, i.e. towards smaller optical depth. Being compressed between inward and outward moving layers, a region of heating is anticipated, represented by $\Delta T(\tau)$.

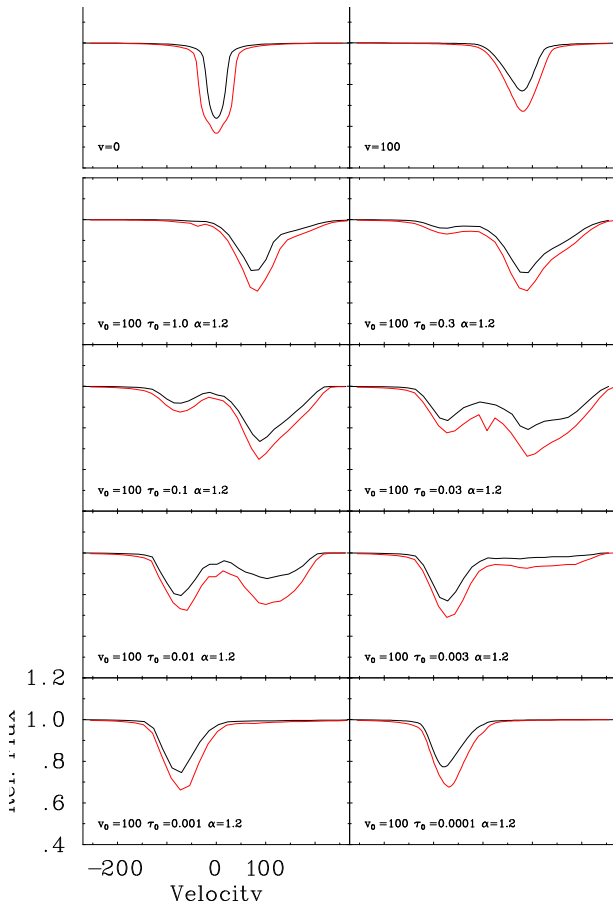


Figure 11.2: Normalised line profiles for He I 6678 and 5876 (solid/black, dashed/red, respectively) for a standard model atmosphere in which the local velocity $v(\tau)$ is specified, with τ_0 running from ∞ (uniform contraction) through to 0 (uniform expansion) and $v(0) = -v(\infty) = 100 \text{ km s}^{-1}$ (as in Fig. 11.1). The extent of the transition layer is given by $\alpha = 1.2$. The top two panels represent the stationary atmosphere (left) and the uniformly contracting atmosphere (right). To compare with the passage through minimum radius, the subsequent panels progress in sequence left to right (as in lines of text).

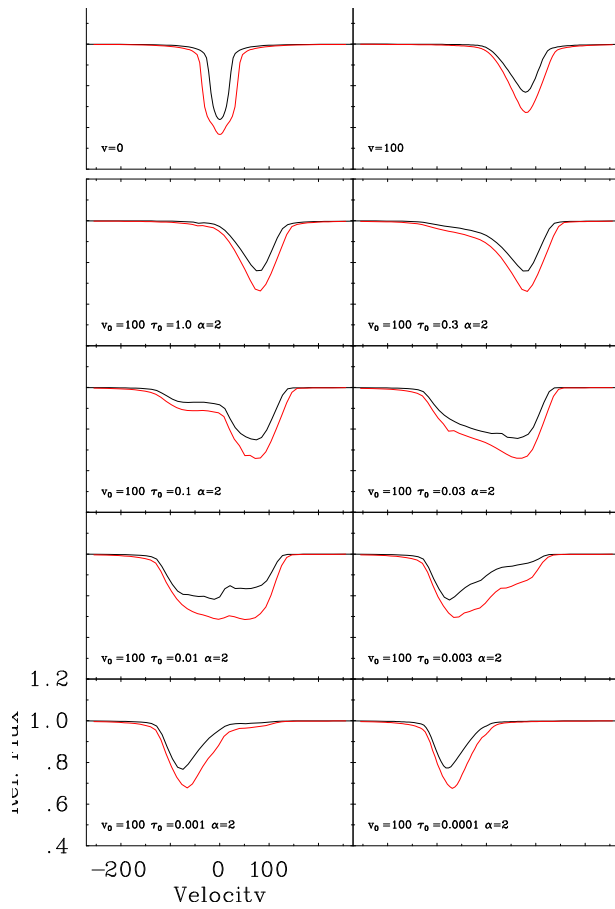


Figure 11.3: As Fig. 11.2 with $\alpha = 2$, representing a sharper transition layer between inward and outward moving layers..

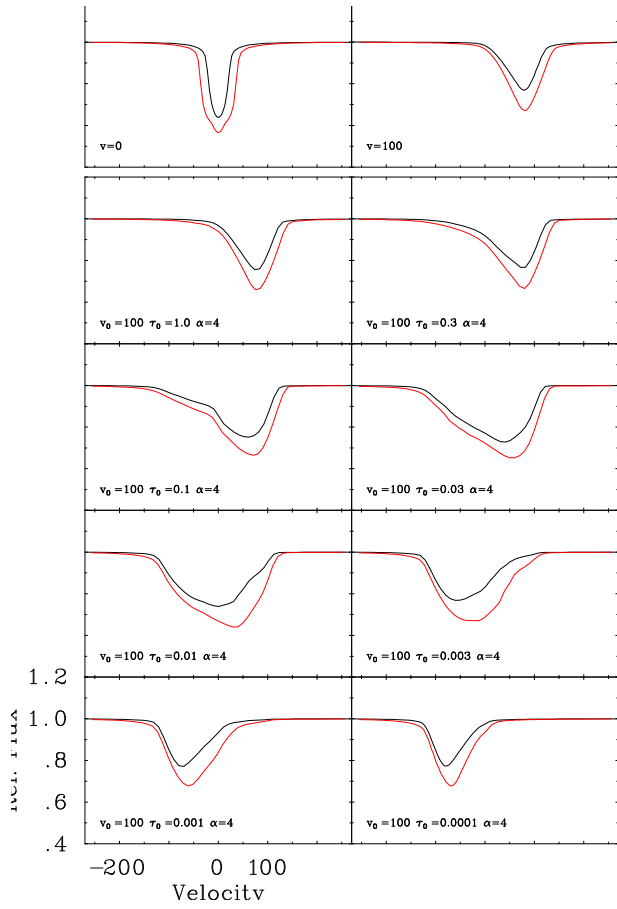


Figure 11.4: As Fig. 11.2 with $\alpha = 4$, representing a broader transition layer between inward and outward moving layers..

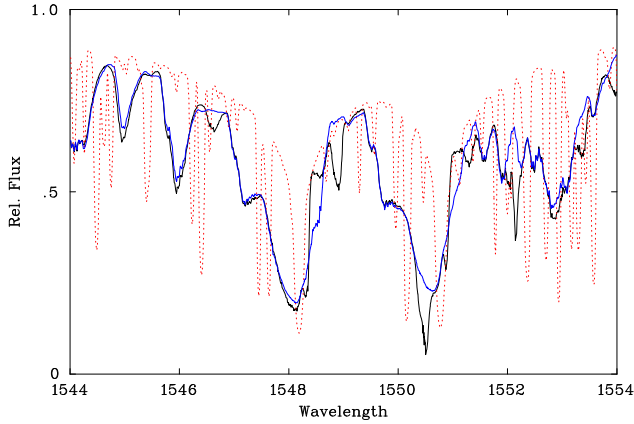


Figure 11.5: Normalised spectra in the region of Civ1548,1550 with $v_0 = 50$, $\tau_0 = 0.1, 0.03$ and $\alpha = 4$ (solid and dashed lines) and with $v = 0$ (dotted line). This figure is available in colour in the online version of the journal on *Synergy* where the profiles for $\tau_0 = 0.1$ and 0.03 are shown black and blue, respectively. The profile with $v = 0$ is red.

Note that $\alpha = 1$ corresponds to a discontinuity and increasing α corresponds to increasing the extent of the transition layer.

To simulate passage through minimum radius, the stationary point has been moved through a series of optical depths from $\tau_0 = \infty, 1.0, 0.3, 0.1, 0.03, 0.01, 0.003, 0.001, 0.0001$. For simplicity $v(\infty) = -v(0)$, and $v(0) = 100 \text{ km s}^{-1}$ have been used throughout, although some experimental calculations were made with $v(0) = \pm 50$ (units of km s^{-1} should be assumed for v hereafter). We have investigated models with $\alpha = 1.2, 2$ and 4 .

HeI 5876,6678

Figures 11.2, 11.3 and 11.4 show profiles for two strong HeI lines as a function of different velocity structures. The temperature and density structures are unperturbed. The line profiles for trivial cases (cf. ?) include the stationary atmosphere corresponding roughly to maximum radius (Fig. 11.2: $v = 0$) and a uniformly moving atmosphere (Fig. 11.2: $v = 100$) and demonstrate that the basic radiative transfer calculations are operating correctly.

As the stationary point is moved from large optical depth toward smaller depths, simulating a progressive reversal of the atmospheric motion, the line profile initially resembles the uniformly contracting case ($v_0 = 100, \tau_0 = 1.0$). It starts to develop a blue component, when $\tau_0 \leq 0.3$, and finally loses the red component when $\tau_0 \leq 0.001$, where it closely resembles the uniformly expanding case (not shown).

The extent of the transition layer, represented by α , is clearly important. For $\alpha = 1.2$, line splitting is readily apparent as the stationary point traverses the line forming region at $0.1 > \tau_0 > 0.01$. In this case the steep velocity gradient means that the broader line forming region includes both inward and outward moving material. For larger α , the distinction between the two components is reduced, as a larger fraction of the line forming region lies at intermediate velocities.

A comparison of these profiles with observation allows us to approximately identify the best values of τ_0 and α at a particular phase. We emphasize, however, that in this purely parametric representation of the velocity structure, α is likely to vary with τ_0 .

For this initial set of models, it is considered that the profile of HeI6678 most closely resembles that of BW Vul at phase $\phi \approx 0.90$ (? Fig. 7), for the case with $\tau_0 = 0.03$ and $\alpha = 4$. This is essentially the optical depth at which the line cores are formed. With $\alpha = 4$, the transition layer extends from $\tau = 0.0075 - -0.12$. Since blue-shifted absorption arises at optical depths $\tau > \tau_0$, the effect of increasing α , in this case, is to reduce the amount of moving material contributing to the total line absorption.

It will be seen that in all of these models, the behaviour of HeI6678 and 5876 mimic each other quite closely. There is no evidence of an additional blue-shifted absorption component appearing in HeI5876 in advance of the blue absorption in HeI6678, as is observed in BW Vul.

There are two conclusions to be drawn. Firstly, it *is* possible to obtain line splitting in the presence of a steep velocity gradient without recourse to density or temperature perturbations. However, the behaviour of BW Vul, where the blue-shifted absorption appears in HeI5876 *before* it appears in HeI6678 cannot be correctly reproduced in this manner. The atmospheric structure must be modified in some other way.

11.1.2. Temperature Perturbations

Temperature perturbations are introduced by a factor β representing the heating at a specified optical depth τ_S , and a width $2\Delta\tau_S$ over which the material is heated by this factor.

Initial investigations have been carried out with $\beta = 0.9$ (cooling) and 1.1, with $\tau_S = 0.001, 0.01, 0.02, 0.03, 0.05$ and 0.1, and with $\Delta\tau_S/\tau_S = 0.05$ and 0.1. As might be expected, significant perturbations in the line profiles are only apparent when the heated or cooled region lies within the line-forming region with, specifically, $0.02 \leq \tau_S \leq 0.05$.

HeI 5876, 6678

Fig. ?? shows profiles for two strong HeI lines as a function of different temperature structures, assuming a velocity structure as defined above with $\tau_0 = 0.03$, $\alpha = 4$ and $v(0) = 100$. Thus the stationary point in the atmosphere is at optical depth $\tau = 0.03$. With $\alpha = 4$, material at $\tau < 0.0075$ is moving at maximum infall velocity $v(0)$. Below this, i.e. at $\tau > 0.0075$, material is being accelerated outwards down to $\tau = 0.12$ where maximum outflow velocity is achieved. If $\tau_S = 0.03$, heated material produces *more* absorption at the line centre. Cooled material not only produces less line absorption in a given layer, but also reduces the total opacity in that layer. The emergent flux then originates in deeper and hotter layers than normally visible, appearing in one case ($\tau_S = 0.1$) as emission. If $\tau_S > 0.03$, this excess absorption (or emission) will be blueshifted. Conversely, if $\tau_S < 0.03$ it will be redshifted.

The desired result involves excess blue-shifted absorption, corresponding to heating *below* the standstill point in the atmosphere.

Bibliography

- Barnard A. J., Cooper J., Shamey L. J., 1969, A&A, 1, 28
- Barnard A. J., Cooper J., Smith E. W., 1974, J. Quant. Spec. Radiat. Transf., 14, 1025
- Barnard A. J., Cooper J., Smith E. W., 1975, J. Quant. Spec. Radiat. Transf., 15, 429
- Beauchamp A., Wesemael F., Bergeron P., 1997, ApJS, 108, 559
- Behara N. T., Jeffery C. S., 2006, A&A, 451, 643
- Behara N. T., Jeffery C. S., 2007, in Napiwotzki R., Burleigh M. R., eds, 15th European Workshop on White Dwarfs Vol. 372 of Astronomical Society of the Pacific Conference Series, Self-Consistent Diffusion in Low Mass Hot Stars. pp 213–+
- Berrington K., 1995, in Adelman S. J., Wiese W. L., eds, ASP Conf. Ser. 78: Astrophysical Applications of Powerful New Databases Summary of the Iron and Opacity Projects. pp 19–+
- Gustafsson B., Bell R. A., Eriksson K., Nordlund A., 1975, Å, 42, 407
- Heber U., 1983, A&A, 118, 39
- Heber U., Hunger K., Jonas G., Kudritzki R. P., 1984, Å, 130, 119
- Heber U., Schoenberner D., 1981, Å, 102, 73
- Jeffery C. S., 1989, QJRAS, 30, 195
- Jeffery C. S., Heber U., 1992, A&A, 260, 133
- Jeffery C. S., Woolf V. M., Pollacco D. L., 2001, A&A, 376, 497
- Kurucz R. L., 1970, SAO Special Report, 309
- Lemke M., 1997, A&AS, 122, 285
- Möller R. U., 1990, Master's thesis, Universität Kiel
- Napiwotzki R., 1997, A&A, 322, 256
- Pandey G., Lambert D. L., Jeffery C. S., Rao N. K., 2006, ApJ, 638, 454

Peach G., 1970, MmRAS, 73, 1

Peytremann E., 1974, å, 33, 203

Przybilla N., Butler K., Heber U., Jeffery C. S., 2005, A&A, 443, L25

Schönberner D., 1975, A&A, 44, 383

Schönberner D., Wolf R. E. A., 1974, A&A, 37, 87

Schöning T., Butler K., 1989, A&AS, 78, 51

Seaton M. J., Yan Y., Mihalas D., Pradhan A. K., 1994, mnras, 266, 805

Shulyak D., Tsymbal V., Ryabchikova T., Stütz C., Weiss W. W., 2004, å, 428, 993

Tarafdar S. P., Vardya M. S., 1969, mnras, 145, 171

Vidal C. R., Cooper J., Smith E. W., 1973, ApJS, 25, 37

Walker H. J., Schönberner D., 1981, A&A, 97, 291



SPECTRUM - command summary

A.1. General Commands

echo [off | 0 | 1 | 2 | on] : adjust i/o level

debug [mn | wh | ln | op | at | md | ou | ot] : adjust debug level

check : confirm settings

qub : original version – use numerical options (deprecated)

end, exit, q : finish work

A.2. Parameter Definition

nsource $\langle n \rangle$: choice of source function (def: 3=Feautrier)

noptype $\langle n \rangle$: choice of continuous opacity (def: 1=Kiel)

nhedat $\langle nhedat \rangle$: choice of HeI data (BCS or Mon treat) (def: 1=BCS)

nhestark $\langle nhestark \rangle$: choice of HeI Stark coefficients (def: 2)

ntheta $\langle ntheta \rangle$: number of angles for specific intensity (def: 0)

costheta $\langle \mu_1, \mu_2, \mu_3, \dots, \mu_n \rangle$: list of cosine angles for intensities

costmin $\langle \mu_{\min} \rangle$: minimum cosine angles for intensity

nmode $\langle nmode \rangle$: mode of operation – Redundant

A.3. Model Atmosphere Input

read_model $\langle filename \rangle$: read model atmosphere in QUB/STERNE2 format

read_sterne $\langle filename \rangle$: read model atmosphere in STERNE3 format

read_hydro $\langle filename \rangle$: read model atmosphere in one set of hydrodynamic scalings

A.4. Atomic Data

read_lines $\langle filename \rangle$: read in linelist
line_threshold $\langle value \rangle$: reject lines weaker than $\sim??$ mÅ
wavmax $\langle w_{max} \rangle$: distance from line centre to compute
wtol $\langle w_{tol} \rangle$: identify lines and blends within this tolerance

A.5. Abundances

abund $\langle z \rangle \langle n_z \rangle$: element abundance
abfrac $\langle z \rangle \langle n_z \rangle$: fractional abundance for element
ablog $\langle z \rangle \langle n_z \rangle$: log fractional abundance for element
abmodel : define abundances from input model
 Default for all elements – solar abundance. All elements scaled to iron unless specified explicitly.

A.6. Velocities, etc.

vturb $\langle v_{turb} \rangle$: microturbulent velocity (km/s)
nvturb $\langle n_{vt} \rangle$: number of points in τ -dependent v_{turb}
vtrb_tau see help : values of τ, v_{turb} for τ -dependent v_{turb}
vrad $\langle v_{rad} \rangle$: radial velocity (km/s)
nvr $\langle n_{vr} \rangle$: number of points in τ -dependent v_{rad}
vrad_tau see help : values of τ, v_{rad} for τ -dependent v_{rad}
tau_exp $\langle n \rangle$: increase resolution of optical depth scale by adding additional points
tauscale $\langle n_\tau \rangle$ see help: rescale the optical depth scale using $\langle n_\tau \rangle$ new depth points
taulogs $\langle n_\tau \rangle$ see help: rescale the optical depth scale using $\langle n_\tau \rangle$ new depth points given as logs

A.7. Radiative Transfer

calc_prof $\langle z \rangle \langle wl \rangle \langle ab \rangle \langle v_t \rangle$: compute line profile for single line or blend
calc_abund $\langle z \rangle \langle wl \rangle \langle ew \rangle \langle v_t \rangle$: compute abundance from equivalent width
calc_synth $\langle w_{min} \rangle \langle w_{max} \rangle$: compute synthetic spectrum in given wavelength interval
calc_lines $\langle w_{min} \rangle \langle w_{max} \rangle$: compute equivalent widths for all lines in given wavelength

interval

A.8. Examples

[Examples](#)

B

ltercodes – walkthrough examples

Chapter author: James Wild

B.1. example.spc

```
echo 2
nsource 3
nhedat 2
read_model
read_lines
nopetype 2

vturb 2
line_threshold 0.0

!Optical
abund 1 11.699
abund 2 11.022
abund 6 8.609
abund 7 8.023
abund 16 7.809
abund 18 8.300
abund 20 7.734
abund 21 7.750
abund 22 7.754
abund 23 8.400

calc_lines 3900 6900
```

end

B.2. StnPG0909

```
#!/bin/bash
#####
# PG0909+276
# Sterne_Condor grid teff logg nH nHe c n o si ca fe mix
star=pg0909n276 # this is used for the folder label

# default mixture
nhh=0.85 # number fraction
nhe=0.15 # number fraction
nc=0.003 # number fraction
nn=0.0001 # number fraction
no=0.1 # times solar
nsi=0.05 # times solar
nca=30 # times solar
nfe=3000 # times solar

vt=5 # microturbulent velocity.
mix=pg0909 # a label for the mixture which goes on the folder and file names.
teffs="260 280 300 320 340 360 380 400 420"
gravs="5.00 5.25 5.50 5.75 6.00"

for ab in ${mix}; do
  if [ ! -e ${star}_${ab} ]; then mkdir ${star}_${ab}; fi
  for tt in ${teffs}; do
    for gg in ${gravs}; do
      if [ ! -e GenGrid.Job ]; then mkdir GenGrid.Job; fi
      if [ ! -e GenGrid.Log ]; then mkdir GenGrid.Log; fi
      if [ "$1" == "clean" ]; then rm GenGrid.Job/* GenGrid.Log/* ; fi
      # Construct the files, and fill it with the condor job,
      glab=${gg}/./}
      label="${star}.t${tt}g${glab}${ab}"
      echo Sterne_Batch `pwd` ${star}_${ab} ${tt} ${gg} $nhh $nhe $nc $nn $no $nsi
        $nca $nfe $vt ${ab}
      # Create the condor job parameters
      cat > ./GenGrid.Job/sterne.${label}.condor <<%%
#####
## Sterne.condor
```

```
#####
executable = /home/csj/bin/Sterne_Batch
universe = vanilla
arguments = `pwd` ${star}_${ab} ${tt} ${gg} $nhh $nhe $nc $nn $no $nsi $nca
           $nfe $vt ${ab}
output = ./GenGrid.Log/sterne.${label}.out
error = ./GenGrid.Log/sterne.${label}.err
log =    ./GenGrid.Log/sterne.${label}.log
queue
%%
    echo "condor_submit GenGrid.Job/sterne.${label}.condor"
    condor_submit GenGrid.Job/sterne.${label}.condor
done
done
done
```

B.3. SpcPG0909

```
#!/bin/bash
#####
# SpcPG0909
#####
star=pg0909n276
mix="p05 p10 p15 p20 p25 p30"

teffs="260 280 300 320 340 360 380 400 420"
gravs="5.00 5.25 5.50 5.75 6.00"
vt=5
wr="opt" # "fuv nuv opt"
root=`pwd`
#####
for ab in ${mix}; do
  grd=${star}_${ab}
  ls
  cd ${grd}; pwd
  for tt in ${teffs}; do
    for gg in ${gravs}; do
      # Check that the log files exist, and if they dont then create them
      if [ ! -e GenGrid.Job ]; then mkdir GenGrid.Job; fi
      if [ ! -e GenGrid.Log ]; then mkdir GenGrid.Log; fi
      if [ "$1" == "clean" ]; then rm GenGrid.Job/spectrum* GenGrid.Log/spectrum*
        ; fi

      # Construct the file, and then cat the commands to it
      glab=${gg}/.}
      label="${star}.t${tt}g${glab}${ab}v${vt}"
      model="t${tt}g${glab}${ab}"
      if [ ! -e ${model}.q ]; then echo "Model ${model}.q not found"; continue; fi
      if [ -e ${model}.000 ]; then echo "Model ${model}.000 exists"; continue; fi
      echo Spectrum_Batch `pwd` ${model}.q ${root}/gf_opt.lte
        ${root}/opt_${ab}_v${vt}.spc ${model}
      cat > GenGrid.Job/spectrum.${label}.condor <<%%
#####
## spectrum.condor
#####
```

```
executable = /home/csj/bin/Spectrum_Batch
universe = vanilla
arguments = `pwd` ${model}.q ${root}/gf_${wr}.lte
           ${root}/${wr}_${ab}_v${vt}.spc ${model}.${wr}
output = GenGrid.Log/spectrum.${label}.out
error = GenGrid.Log/spectrum.${label}.err
log =    GenGrid.Log/spectrum.${label}.log
queue
%%
  # Submit the job for computing
  condor_submit GenGrid.Job/spectrum.${label}.condor
done
done
cd ..
done
```

B.4. sterneos.sh

A copy of this script can be found on [my github](#)

```
#!/bin/bash
#
# SterneOS - Take a Sterne data file and input it into Sterne,
#   generating a model atmosphere
#
# Authors:
#   C. Simon Jeffery (csj@arm.ac.uk) - Original csh version
#   Chris Winter (cwr@arm.ac.uk) - Bourne sh version
#
###
# How to use this script
print_usage()
{
    echo ""
    echo "SterneOS - Usage Information"
    echo "======"
    echo ""
    echo "SterneOS [star_data [odf [int [model] ] ] ]"
    echo ""
}
###
# Ask user for Sterne star data file (generated by Sterne.input)
###
get_star_data()
{
    echo -n 'File containing sterne input: '
    read DATA
}
###
# Check that star_data file exists. Possibly grep the content
# to make sure the file specified has been generated by SterneOS.input
###
check_star_data()
{
    # Set to zero just in case
    DATA_ERROR=0
}
```

```

# While file $DATA doesn't exist and $DATA_ERROR < 5
while [ -z "$DATA" -a ! -r "$DATA" -a "$DATA_ERROR" -lt 5 ]
do
    echo -n "Can't find $DATA. Please try again: "

    read DATA
    DATA_ERROR=`expr $DATA_ERROR + 1`
done

if [ "$DATA_ERROR" -ge 5 ]
then
    # Something is wrong. Bail out
    echo "Number of attempts exceeded. Exiting..."
    clean_up
    exit 1
fi

DATA_EX=`basename $DATA` # Strip off any extension
}
###
# Ask user for the opacity distribution function(s) file
###
get_odf()
{
    echo -n "File containing ODF(s) (<CR> for continuum models): "
    read ODF
}
###
# Check if the user has specified a file that actually exists
###
check_odf()
{
    # $ODF of zero length?
    if [ -z "$ODF" ]
    then
        echo "Calculating continuum model"
    else
        # Set to zero just in case
        ODF_ERROR=0
    fi
}

```

```
# While file $ODF doesn't exist and $ODF_ERROR < 5
while [ ! -r "$ODF" -a ! -r "$GLOBAL_DATA/odf6/$ODF" -a "$ODF_ERROR" -lt
  5 ]
do
  echo -n "Can't find $ODF. Please try again: "
  read DATA
  ODF_ERROR=`expr $ODF_ERROR + 1`
done

if [ "$ODF_ERROR" -ge 5 ]
then
  # Something is wrong. Bail out
  echo "Number of attempts exceeded. Exiting..."
  clean_up
  exit 1
else
  # Check where we found the file and assign variable $DF
  DF="$GLOBAL_DATA/odf6/$ODF"

  if [ -r "$ODF" ]
  then
    DF="$ODF"
  fi
  echo "Opacity distribution function: " $DF
fi
fi
}
###
# As the user for the interval: BIG or LIT
###
get_interval()
{
  echo -n "BIG or LIT intervals (<CR> for default BIG): "
  read INT
}
###
# Check if user's input was valid
###
check_interval()
{
```

```
# OS grid:
WL="grid05-500-1-900-25-5000.d"

# Did user enter 'LIT' instead?
if [ "$INT" = "LIT" -o "$INT" = "int" ]
then
    WL="wavekurl.d"
fi

}
###
# As user if they want to restart a model, and if so, what
# that model's file name is
###
get_model()
{
    echo -n "File containing start model: "
    read MODEL
}
###
# Check that the model exists
###
check_model()
{
    if [ -z "$MODEL" ]
    then
        MODEL="$DATA_EX.MODEL"
    fi

    echo "Input/output model: " "$MODEL"
    echo "$DATA_EX " > name

    # Tidy up old files
    if [ -e "$DATA_EX.output" ]
    then
        mv "$DATA_EX.output" "$DATA_EX.output%"
    fi
}
###
# Ask user to input paramters
```

```
###
get_params()
{
    get_star_data
    check_star_data
    get_odf
    check_odf
    get_interval
    check_interval
    get_model
    check_model
}
###
# Check if Sterne is actually installed, and look for
# the global data folder
###
sanity_check()
{
    # Try looking in LTECODES environment variable
    STERNE=$LTECODES/bin/sterneOS

    if [ ! -x "$STERNE" ]
    then
        # Does whereis know where Sterne is? (i.e. is sterne
        # in /usr/local/bin/sterne)
        WHEREIS=`whereis sterneOS | awk '{print $2}'`

        if [ -x "$WHEREIS" ]
        then
            STERNE="$WHEREIS"
        else
            echo "Can't find Sterne. Please set the LTECODES environment"
            echo "variable as described in the installation instructions."
            echo "Exiting..."
            exit 1
        fi
    fi

    # Now to look for the data directory
    # Set to null just incase
```

```

GLOBAL_DATA=""

# First, check in the default locations
#
# $LTECODES/share/osdata - Environment variable
# /usr/local/share/osdata - The default installer location
# /usr/local/osdata - Possible secondary location
# /usr/osdata - Possible secondary location
# /opt/osdata - Possible secondary location
# ~/ - Check user's home directory
# ./osdata - Check current directory
# ../osdata - Getting desperate
# ../../osdata - Very desperate
# ./lines - Last chance effort - check if we're
# actually *in* osdata
for i in \
    $LTECODES/share/osdata \
    /usr/local/share/osdata \
    /usr/local/osdata \
    /usr/osdata \
    /opt/osdata \
    ~/osdata \
    ./osdata \
    ../osdata \
    ../../osdata \
    ./lines \
do
    # Is this it?
    if [ -d "$i" ]
    then
        GLOBAL_DATA="$i"

        # Ok, the last case in for loop is special
        # so check for it
        if [ "$i" = "./lines" ]
        then
            GLOBAL_DATA=./
        fi

        # We've found the location, so break out of loop

```

```
        break
    fi
done

# Was our search successful?
if [ ! -d "$GLOBAL_DATA" ]
then
    echo "Can't find the global data directory. Please set the LTECODES"
    echo "environment variable as described in the installation"
    echo "instructions. Exiting..."
    exit 1
fi
}
###
# Validate the user's parameters
###
check_params()
{
    case "$#" in
        "0")
            get_params
            ;;
        "1")
            DATA=$1
            ;;
        "2")
            DATA=$1
            ODF=$2
            ;;
        "3")
            DATA=$1
            ODF=$2
            INT=$3
            ;;
        "4")
            DATA=$1
            ODF=$2
            INT=$3
            MODEL=$4.MODEL
            ;;
    esac
}
```

```

        *)
        print_usage
        exit 1
        ;;
    esac

    check_star_data
    check_odf
    check_interval
    check_model
}
setup_links()
{
    # Link for interval
    ln -fs $GLOBAL_DATA/spectrum_data/$WL WAVE

    # Link for ODF - only if not continuum
    if [ ! -z "$ODF" ]
    then
        ln -fs $DF fort.10
    fi

    # Data Links
    # First link looks for Spectrum data folder
    ln -fs $GLOBAL_DATA/opacity/op_mono OPDATA
    ln -fs $GLOBAL_DATA/opacity/fe_op FEDATA
    ln -fs $GLOBAL_DATA/spectrum_data/peach_tables PEACH_TABLES
    ln -fs $GLOBAL_DATA/spectrum_data/gfall_hout_toPaschen LINELIST

    # Input/Output Links
    ln -fs $MODEL MODIN

    ln -fs $DATA_EX.2 fort.2
    ln -fs $DATA_EX.3 fort.3
    ln -fs $DATA_EX.MODEL STN_MODEL
    ln -fs $DATA_EX.MOD STN_MOD
    ln -fs $DATA_EX.q STN_q
    ln -fs $DATA_EX.s STN_s
    ln -fs $DATA_EX.t STN_t
}

```



```
run_program()
{
    echo ""
    echo "Running program..."
    echo ""

    if [ "$#" -eq "0" ]
    then
        $STERNE <$DATA
    else
        $STERNE <$DATA >"$DATA_EX".output
    fi
}
###
# Tidy up the links
###
clean_up()
{
    rm -f PEACH_TABLES WAVE name fort.10 MODIN STN_MOD STN_MODEL fort.2 fort.3
        STN_q STN_s STN_t OPDATA
}
###
# Tidy up the links then exit
###
clean_up_exit()
{
    clean_up
    exit 1
}
###
# Main program
###
# Tidy-up mode - Backwards compatibility feature
if [ "$1" == "clean" ]
then
    clean_up
    exit 0
fi

# Catch any Ctl^C interrupts
```

```
trap clean_up_exit 2

### Variables
DATA="" # star_data filename
DATA_EX="" # star_data filename minus any extension (Used to create output
           files, etc)
DATA_ERROR=0 # Error counter - reading star_data filename

INT="" # Interval
WL="" # Full path to interval data      !!!!! FIX ME !!!!! (This right?)

ODF="" # File containing opacity distribution function
DF="" # Full path to ODF file
ODF_ERROR=0 # Error counter when reading in ODF filename

MODEL="" # File containing model to restart from

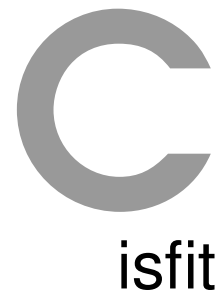
STERNE="" # Path to Sterne executable
STERNE_ERROR=0 # Error counter when asking Sterne location

GLOBAL_DATA="" # Where the data files are installed
GD_ERROR=0 # Error counter when asking for osdata

sanity_check # Is the environment brain damaged?

check_params $@
setup_links
run_program $@
clean_up

exit 0
```



Author: Gustavo Dopcke 2003

isfit is a Interface for **sfit** made in Java which join two basic tools. One is the **sfit** Control File Editor that control the initial values for the **sfit** variables, the the model grid and the observed spectrum. The other tool is for opening the **sfit** output file.

C.1. sfit control file editor

The Control File Editor is the tool that permits the user choose the parameters for **sfit**.

Model Grid

The first parameter is the model grid, that the user has just to choose the file name containing the model grid.

Spectrum to Fit

The second parameter is the spectrum to fit, where the user choose the spectrum file, sigma, instrument, t and drift. Sigma means the standard error on data in 'spectrum', instrument is the FWHM (A) of instrumental broadening function, cosmic is the threshold for rejection of fluxes (e.g. due to cosmic ray spikes) and drift means velocity drift (km/s) during exposure.

Fitting Method

levenburg, amoeba, genetic or chi-squared), for each method the user has to choose the range and the method tolerance.

levenburg Levenburg-Marquardt method
amoeba & Downhill simplex method
genetic & Genetic algorithm
chi-squared & Compute chi-squared surface only
range w1 w2 & Wavelength region to include in fit
tolerance & Convergence criterion

If the genetic algorithm is chosen the user has to fill the genetic parameters that are in the table above.

Parameter	Meaning	Default	Allowed
Generations	The maximum number of generations the program will go through, before stopping, if the solution is not within the given tolerance.	10	
Population	The number of parents randomly generated in the first generation, and in each subsequent generation.	50	
Probability of mutation	The probability of mutation in the offspring.	0.02	0 - 1
Probability of crossover	The probability of crossover between two parents.	0.8	0 - 1
Tolerance	The highest suitability which will be tolerated.	1	
Selection Method	There are three selection methods available: tournament, rank, and fitness proportionate.	Rank	rank tournament fitness
Contestants	Specific to tournament selection. This number of parents will be selected at random and from these the two with the lowest chi-squared values will be chosen as a pair of parents.	10	
Substring Length	Defines the number of characters coding each parameter. This is multiplied by the number of parameters being varied to give the total string length for each parent.	16	
Alphabet Size	The number of different characters encoding the parent. For instance if this variable is given the value 2 the parent will be encoded by a string of ones and twos	3	
Elitism	An option which, if set to 'yes', always keeps the best few members of each generation.	No	yes no
Kept	Only required if elitism is selected. Defines the number of individuals to be carried over to the next generation (if elitism is selected).	3	

Parameters

The parameters for starting the fit have to be given for **sfit** to calculate the best fit. Define the initial parameters to be used by solve. The parameters are:

For the primary:

- Effective temperature. $T_{\text{eff}}/1000\text{K}$
- Surface gravity (log cgs)
- Surface composition parameter that depends on model grid
- Projected rotation velocity (km/s)
- Radial velocity (km/s)
- Brightness contribution

For the secondary:

- Effective temperature for secondary. $T_{\text{eff}}/1000\text{K}$
- Surface gravity (log cgs)
- Surface composition parameter that depends on model grid
- Projected rotation velocity (km/s)
- Radial velocity (km/s)
- Brightness contribution

If there is only one spectrum to fit, one should set default parameters for the secondary which lie within the model grid, with Brightness contribution being a very small value.

Mask

Define regions to exclude from fit. Example: to emphasize He, Si and Mg cores in fit, excluding the other regions.

Go

The “go button” starts **sfit** fitting and opens, in the plotter tool, the observational spectrum and the theoretical fitted by **sfit**.

C.2. Plot sfit output

The Plot Output **sfit** File is a tool created for plotting the observational spectrum and the theoretical one, these two are in the **sfit** output file. The observational spectrum is plotted in red and the theoretical one is in blue. It shows the parameters for the model shown on the left.

Menu File

There are four options in the menu file: Open, Save, Export and Close.

Open is for opening a spectrum in **sfit** output format.

Save is for saving the plot in a image file.

Export is for exporting the plot in EPS format.

Close is for exiting the plot tool.

Menu Operations

Five operations are available.

Set Plot Format is used for setting the vertical and horizontal ranges, the grid, the title and the labels.

Restore is for reset the rangens for the amplitudo of the spectrum.

Print is for sendin the plot for the printer.

The Refresh option is used when reading the file again is necessary, like when the **sfit** is runned and change the points in the theoretical spectrum.

Show Parse Informations is checked when the user want to see the informations about the star and hidden when the user want more space for the plot on the screen.

The buttons on the top-right of the screen have the same function like the operations commands.

C.3. Examples

LSS 1922

Get the best fit for LSS1922 using the model grid “modelexample”. It is allowed to vary the Temperature and the gravity, the two searched values.

The spectrum file is “aat02_lss1922.sp2” and the model grid cover temperatures between 10 and 14 KiloKelvins and gravities between 0 and 1.5 cgs.

After filling the values and clisk in the “Go” button the Plot Tool will open the observational spectrum and the theoretical spectrum.

LSS 4300

Now, the stellar spectrum is “wht96_iss4300_blue.sp2” relative to the star LSS 4300 and the model grid will be the same, but now some regions will be masked for excluding less-relevant parts of the spectrum for finding the best fit.

The parameters allowed to vary are the Temperature, the Gravity and the Radial Velocity. These are shown in the Plot tool.

After filling the values and click in the “Go” button the Plot Tool will open the observational spectrum and the theoretical spectrum.